ASC Report No. 34/2014

Adaptive boundary element methods for optimal convergence of point errors

M. Feischl, T. Führer, G. Gantner, A. Haberl, D. Praetorius

Institute for Analysis and Scientific Computing —
Vienna University of Technology — TU Wien
www.asc.tuwien.ac.at ISBN 978-3-902627-05-6

Most recent ASC Reports

33/2014 *M. Halla, L. Nannen*
Hardy space infinite elements for time-harmonic two-dimensional elastic waveguide problems

32/2014 *A. Feichtinger and E. Weinmüller*
Numerical treatment of models from applications using BVPSUITE

31/2014 *C. Abert, M. Ruggeri, F. Bruckner, C. Vogler, G. Hrkac, D. Praetorius, and D. Suess*
Self-consistent micromagnetic simulations including spin-diffusion effects

30/2014 *J. Schöberl*
C++11 Implementation of Finite Elements in NGSolve

29/2014 *A. Arnold and J. Erb*
Sharp entropy decay for hypocoercive and non-symmetric Fokker-Planck equations with linear drift

28/2014 *G. Kitzler and J. Schöberl*
A high order space momentum discontinuous Galerkin method for the Boltzmann equation

27/2014 *W. Auzinger, T. Kassebacher, O. Koch, and M. Thalhammer*
Adaptive splitting methods for nonlinear Schrödinger equations in the semiclassical regime

26/2014 *W. Auzinger, R. Stolyarchuk, and M. Tutz*
Defect correction methods, classic and new (in Ukrainian)

25/2014 *J.M. Melenk and T.P. Wihler*
A posteriori error analysis of hp-FEM for singularly perturbed problems

24/2014 *J.M. Melenk and C. Xenophontos*
Robust exponential convergence of hp-FEM in balanced norms for singularly perturbed reaction-diffusion equations

Institute for Analysis and Scientific Computing
Vienna University of Technology
Wiedner Hauptstraße 8–10
1040 Wien, Austria

E-Mail: admin@asc.tuwien.ac.at
WWW: http://www.asc.tuwien.ac.at
FAX: +43-1-58801-10196

ISBN 978-3-902627-05-6

ASC TU WIEN

ADAPTIVE BOUNDARY ELEMENT METHODS FOR OPTIMAL CONVERGENCE OF POINT ERRORS

M. FEISCHL, T. FÜHRER, G. GANTNER, A. HABERL, D. PRAETORIUS

Abstract. One particular strength of the boundary element method is that it allows for a high-order pointwise approximation of the solution of the related partial differential equation via the representation formula. However, the high-order convergence and hence accuracy usually suffers from singularities of the Cauchy data. We propose two adaptive mesh-refining algorithms and prove their quasi-optimal convergence behavior with respect to the point error in the representation formula. Numerical examples for the weakly-singular integral equations for the 2D and 3D Laplacian underline our theoretical findings.

1. Introduction

For a bounded Lipschitz domain $\Omega \subset \mathbb{R}^d$ with boundary $\Gamma := \partial\Omega$, $d = 2, 3$, we consider the Laplace-Dirichlet problem

$$-\Delta u = 0 \text{ in } \Omega \text{ subject to Dirichlet boundary conditions } u = g \text{ on } \Gamma. \tag{1}$$

with given Dirichlet data $g \in H^{1/2}(\Gamma)$. Note that, away from the boundary Γ, the potential u is smooth, i.e., $u \in C^\infty(\Omega)$. With the simple-layer potential $\widetilde{V}$ and the double-layer potential $\widetilde{K}$, the solution $u \in H^1(\Omega)$ of (1) is pointwise given by the representation formula (or: third Green's formula)

$$u(\widetilde{x}) = \widetilde{V}\phi(\widetilde{x}) - \widetilde{K}g(\widetilde{x}) \quad \text{for all } \widetilde{x} \in \Omega, \tag{2}$$

where $\phi = \partial_n u$ is the unknown normal derivative of u; see Section 2 for this and the following mathematical facts. The unknown normal derivative $\phi = \partial_n u$ can be obtained from the weakly-singular integral equation

$$V\phi(x) = (K + 1/2)g(x) \quad \text{for } x \in \Gamma, \tag{3}$$

where the simple-layer integral operator V and the double-layer integral operator K formally coincide with the volume potentials $\widetilde{V}$ and $\widetilde{K}$, but are now evaluated for $x \in \Gamma$.

For $d = 2$, we assume $\operatorname{diam}(\Omega) < 1$ which can always be achieved by scaling. Then, for $d = 2, 3$, the simple-layer integral operator $V : H^{-1/2}(\Gamma) \to H^{1/2}(\Gamma)$ is a continuous, elliptic, and symmetric linear operator. Therefore, (3) admits a unique solution which can be approximated by the Galerkin boundary element method (BEM). For a conforming mesh $\mathcal{T}_\ell$ of Γ, the latter provides a Galerkin approximation $\Phi_\ell \in \mathcal{P}^p(\mathcal{T}_\ell)$ which is a discontinuous $\mathcal{T}_\ell$-piecewise polynomial of degree $\le p$. Having obtained Φ_ℓ, the representation formula (2) allows to define an approximate solution $u_\ell \in H^1(\Omega)$ of (1) by

$$u_\ell(\widetilde{x}) := \widetilde{V}\Phi_\ell(\widetilde{x}) - \widetilde{K}g(\widetilde{x}) \quad \text{for all } \widetilde{x} \in \Omega. \tag{4}$$

One particular strength of BEM is the possible high-order convergence of $u_\ell(\widetilde{x}) \to u(\widetilde{x})$ for all $\widetilde{x} \in \Omega$. For lowest-order BEM $p = 0$ and a smooth solution ϕ, it holds $\|\phi -$

2000 *Mathematics Subject Classification.* 65N38, 65N50, 41A25, 65Y20.

Key words and phrases. adaptive boundary element method, optimal convergence rates, point error, goal-oriented algorithm.

$\Phi_\ell\|_{H^{-1/2}(\Gamma)} = \mathcal{O}(h_\ell^{p+3/2})$, while $|u(\widetilde{x}) - u_\ell(\widetilde{x})| = \mathcal{O}(h_\ell^{2p+3})$, where h_ℓ denotes the mesh-size of $\mathcal{T}_\ell$. However, these convergence rates are usually spoiled by singularities of the (unknown) solution u and hence lack of regularity.

While earlier works [AFF+13, FKMP13, FFK+14, FFK+13, Gan13] focussed on h-adaptive strategies which aim to recover the optimal rate of convergence of the energy error $\|\phi - \Phi_\ell\|_{H^{-1/2}(\Gamma)}$, the present work proposes and analyzes an optimal adaptive strategy for the pointwise error $|u(\widetilde{x}) - u_\ell(\widetilde{x})|$ for $\widetilde{x} \in \Omega$.

Outline. Section 2 fixes the notation and recalls some necessary preliminaries from the literature. Section 3 formulates two adaptive algorithms (Algorithm 1, Algorithm 3) and states our main result (Theorem 4) which yields optimal convergence for either algorithm. While Algorithm 1 follows ideas from [MS09] and employs a separate Dörfler marking strategy, Algorithm 3 is inspired by [BET11] and uses a combined Dörfler marking instead. In Section 4, we derive some elementary properties of the adaptive algorithms. Section 5 proves Theorem 4 for Algorithm 1, while Section 6 proves Theorem 4 for Algorithm 3. The final Section 7 underlines our theoretical results by 2D and 3D numerical experiments.

2. Preliminaries

This section gives a brief overview on the functional analytic setting of the weakly-singular integral equation (3). For more details, we refer to the monographs [HW08, McL00]. Moreover, a comprehensive discussion on the boundary element spaces employed in the present work can be found in [SS11, Ste08]. Throughout $|\cdot|$ denotes either the Euclidian norm $|z|$ of a vector $z \in \mathbb{R}^d$ or the $(d-1)-$dimensional surface measure $|T|$ of some measurable set $T \subseteq \Gamma$.

2.1. General assumptions and layer potentials. Throughout, we assume that Ω is a bounded Lipschitz domain in $\mathbb{R}^d$, $d = 2, 3$, with polygonal (not necessarily connected) boundary $\Gamma = \partial\Omega$. For $d = 2$, we assume that $\operatorname{diam}(\Omega) < 1$. With the fundamental solution of the Laplacian

$$G(x,y) = -\frac{1}{2\pi} \log|x-y| \text{ for } d = 2 \quad \text{and} \quad G(x,y) = \frac{1}{4\pi} \frac{1}{|x-y|} \text{ for } d = 3, \tag{5}$$

we consider the simple-layer potential $\widetilde{V}$ and the double-layer potential $\widetilde{K}$ defined by

$$\widetilde{V}\phi(\widetilde{x}) = \int_\Gamma G(\widetilde{x}, y)\phi(y)\, ds_y \quad \text{and} \quad \widetilde{K}g(\widetilde{x}) = \int_\Gamma \partial_{n(y)} G(\widetilde{x}, y) g(y)\, ds_y \quad \text{for } \widetilde{x} \in \Omega. \tag{6}$$

These layer potentials give rise to the simple-layer and double-layer integral operators

$$V\phi(x) = \int_\Gamma G(x,y)\phi(y)\, ds_y \quad \text{and} \quad Kg(x) = \int_\Gamma \partial_{n(y)} G(x,y) g(y)\, ds_y \quad \text{for } x \in \Gamma \tag{7}$$

which formally coincide with $\widetilde{V}$ resp. $\widetilde{K}$, but are now evaluated on the boundary Γ.

2.2. Admissible meshes and mesh-refinement. Let $\mathcal{T}$ be a given mesh of Γ into affine line segments resp. flat surface triangles for $d = 2, 3$, respectively. For $d = 3$, we additionally assume that $\mathcal{T}$ is conforming, i.e., hanging nodes are avoided. Moreover, we suppose that $\mathcal{T}$ is generated from a given initial mesh $\mathcal{T}_0$ by a fixed and deterministic mesh-refinement strategy. For 2D BEM, we shall use the 1D bisection algorithm from [AFF+13]. For 3D BEM, we shall use 2D newest vertex bisection; see e.g. [KPP13].

We say that $\mathcal{T}$ is γ-shape regular if

$$\max_{\substack{T,T'\in\mathcal{T}\\ T\cap T'\neq\emptyset}} \frac{\operatorname{diam}(T)}{\operatorname{diam}(T')} \le \gamma < \infty \text{ for } d=2 \text{ and } \max_{T\in\mathcal{T}} \frac{\operatorname{diam}(T)^2}{|T|} \le \gamma < \infty \text{ for } d=3. \tag{8}$$

For any mesh $\mathcal{T}$ and marked elements $\mathcal{M}\subseteq\mathcal{T}$, we let $\mathcal{T}' := \texttt{refine}(\mathcal{T},\mathcal{M})$ be the mesh generated from the mentioned mesh-refinement strategies, i.e., the coarsest mesh, where all elements $T\in\mathcal{M}$ have been bisected and where mesh properties like bounded local mesh-ratio (8) (for 2D BEM [AFF+13]) or conformity and shape regularity (8) (for 3D BEM [KPP13]) are preserved.

We write $\mathcal{T}'\in\texttt{refine}(\mathcal{T})$, if there exist finitely many meshes $\mathcal{T}^{(0)},\dots,\mathcal{T}^{(n)}$ and sets $\mathcal{M}^{(j)}\subseteq\mathcal{T}^{(j)}$ such that $\mathcal{T}=\mathcal{T}^{(0)}$, $\mathcal{T}'=\mathcal{T}^{(n)}$, and $\mathcal{T}^{(j)}=\texttt{refine}(\mathcal{T}^{(j-1)},\mathcal{M}^{(j-1)})$ for all $j=1,\dots,n$, where we formally allow $n=0$, i.e., $\mathcal{T}=\mathcal{T}^{(0)}\in\texttt{refine}(\mathcal{T})$. To abbreviate notation, we let $\mathbb{T} := \texttt{refine}(\mathcal{T}_0)$ be the set of all meshes which can be obtained from the given initial mesh $\mathcal{T}_0$. We note that the chosen mesh-refinement strategies [AFF+13, KPP13] ensure that all $\mathcal{T}\in\mathbb{T}$ satisfy (8), where $\gamma>0$ depends only on $\mathcal{T}_0$.

Finally, we note the following three properties of the mesh-refinement which are used for the quasi-optimality analysis: First, refined elements are bisected into at least two sons, i.e.,

$$\#\mathcal{T} + \#(\mathcal{T}'\backslash\mathcal{T}) \le \#\mathcal{T}' \quad \text{for all } \mathcal{T}\in\mathbb{T} \text{ and all } \mathcal{T}'\in\texttt{refine}(\mathcal{T}). \tag{9}$$

Second, newest vertex bisection [KPP13] as well as the 1D bisection algorithm [AFF+13] guarantee that for all meshes $\mathcal{T},\mathcal{T}'\in\mathbb{T}$, there exists a common refinement $\mathcal{T}\oplus\mathcal{T}'\in\texttt{refine}(\mathcal{T})\cap\texttt{refine}(\mathcal{T}')$ which satisfies

$$\#(\mathcal{T}\oplus\mathcal{T}') \le \#\mathcal{T} + \#\mathcal{T}' - \#\mathcal{T}_0. \tag{10}$$

In fact, the coarsest common refinement for newest vertex bisection as well as 1D bisection is given by the overlay of these meshes. This as well as the overlay estimate (10) are proved in [Ste07] for 2D newest vertex bisection and [AFF+13] for the 1D bisection algorithm. Finally, it has first been observed in [BDD04] for 2D newest vertex bisection that the number $\#\mathcal{T}_\ell$ of elements in $\mathcal{T}_\ell$ can be controlled by the number of marked elements, i.e., for each sequence of meshes $\mathcal{T}_\ell\in\mathbb{T}$ and marked elements $\mathcal{M}_\ell\subseteq\mathcal{T}_\ell$ with $\mathcal{T}_\ell=\texttt{refine}(\mathcal{T}_{\ell-1},\mathcal{M}_{\ell-1})$ for all $\ell\in\mathbb{N}$, it holds

$$\#\mathcal{T}_\ell - \#\mathcal{T}_0 \le C_{\mathrm{mesh}} \sum_{j=0}^{\ell-1} \#\mathcal{M}_j \quad \text{for all } \ell\in\mathbb{N}, \tag{11}$$

where $C_{\mathrm{mesh}}>0$ depends only on $\mathcal{T}_0$. While [BDD04] required an additional assumption on $\mathcal{T}_0$, this assumption has been removed in [KPP13], and $\mathcal{T}_0$ is, in fact, arbitrary. For 1D bisection, where γ-shape regularity is preserved with $\gamma(\mathcal{T}_\ell)\le 2\gamma(\mathcal{T}_0)$ for all $\mathcal{T}_\ell\in\mathbb{T}$, the mesh-closure estimate (11) is shown in [AFF+13]. We note that simple counter examples in [NV12, AFF+13] show that an elementary estimate $\#\mathcal{T}_\ell - \#\mathcal{T}_{\ell-1} \le \widetilde{C}_{\mathrm{mesh}}\#\mathcal{M}_{\ell-1}$ fails to hold for any ℓ-independent constant $\widetilde{C}_{\mathrm{mesh}}>0$.

2.3. Sobolev spaces. Let $L^2(\Gamma)$ and $H^1(\Gamma)$ denote the usual Lebesgue and Sobolev space on $\Gamma=\partial\Omega$. The norm on $H^1(\Gamma)$ reads

$$\|u\|_{H^1(\Gamma)}^2 = \|u\|_{L^2(\Gamma)}^2 + \|\nabla u\|_{L^2(\Gamma)}^2, \tag{12}$$

where $\nabla(\cdot)$ denotes the arc-length derivative (for $d=2$) resp. the surface gradient (for $d=3$). Sobolev spaces of fractional order $0<s<1$ are defined by interpolation

$$H^s(\Gamma) = [L^2(\Gamma), H^1(\Gamma)]_s, \tag{13}$$

where $[\cdot,\cdot]_s$ denotes interpolation by, e.g., the K-method. To abbreviate notation, let $H^0(\Gamma) := L^2(\Gamma)$. The Sobolev spaces $H^{-s}(\Gamma)$ for $0 < s \leq 1$ are defined by duality

$$H^{-s}(\Gamma) = H^s(\Gamma)^*, \tag{14}$$

where duality is understood with respect to the extended $L^2(\Gamma)$-scalar product $\langle \cdot\,,\,\cdot \rangle_{L^2(\Gamma)}$. In particular, it holds $H^{1/2}(\Gamma) \subset L^2(\Gamma) \subset H^{-1/2}(\Gamma)$, where each inclusion is dense and compact. We note that $H^{1/2}(\Gamma)$ is equivalently characterized as the trace space of the Sobolev space $H^1(\Omega)$.

2.4. Integral operators and energy scalar product. The layer potentials (6) define bounded linear operators

$$\widetilde{V} \in L(H^{-1/2}(\Gamma), H^1(\Omega)) \quad \text{and} \quad \widetilde{K} \in L(H^{1/2}(\Gamma), H^1(\Omega)). \tag{15}$$

Moreover, with $\tau : H^1(\Omega) \to H^{1/2}(\Gamma)$ being the (linear and continuous) trace operator, the link between the layer potentials and the boundary integral operators is given through

$$\tau\widetilde{V}\xi = V\xi \quad \text{and} \quad \tau\widetilde{K}v = (K - 1/2)v \quad \text{for all } \xi \in H^{-1/2}(\Gamma) \text{ and } v \in H^{1/2}(\Gamma). \tag{16}$$

Besides the natural stabilities $V \in L(H^{-1/2}(\Gamma), H^{1/2}(\Gamma))$ and $K \in L(H^{1/2}(\Gamma), H^{1/2}(\Gamma))$, it holds

$$V \in L(H^{-1/2+s}(\Gamma), H^{1/2+s}(\Gamma)) \quad \text{and} \quad K \in L(H^{1/2+s}(\Gamma), H^{1/2+s}(\Gamma)) \tag{17}$$

for all $-1/2 \leq s \leq 1/2$, and V is even an isomorphism in this range, since $\Gamma = \partial\Omega$ is closed. Moreover, the simple-layer integral operator is symmetric

$$\langle\!\langle \xi\,,\,\psi \rangle\!\rangle := \langle V\xi\,,\,\psi\rangle_{L^2(\Gamma)} = \langle \xi\,,\,V\psi\rangle_{L^2(\Gamma)} \quad \text{for all } \xi, \psi \in H^{-1/2}(\Gamma) \tag{18}$$

and even elliptic on $H^{-1/2}(\Gamma)$

$$\langle\!\langle \xi\,,\,\xi \rangle\!\rangle = \langle V\xi\,,\,\xi\rangle_{L^2(\Gamma)} \geq C_{\text{ell}}\,\|\xi\|^2_{H^{-1/2}(\Gamma)} \quad \text{for all } \xi \in H^{-1/2}(\Gamma), \tag{19}$$

where $C_{\text{ell}} > 0$ depends only on Ω. Therefore, $\langle\!\langle \cdot\,,\,\cdot \rangle\!\rangle$ is a scalar product on $H^{-1/2}(\Gamma)$, and the induced norm $|\!|\!| \xi |\!|\!|^2 := \langle\!\langle \xi\,,\,\xi \rangle\!\rangle$ is an equivalent norm on $H^{-1/2}(\Gamma)$.

2.5. Weakly-singular integral equation. For any $f \in H^{1/2}(\Gamma)$, the weakly-singular integral equation $V\xi = f$ can equivalently be recast in the variational formulation

$$\langle\!\langle \xi\,,\,\psi \rangle\!\rangle := \langle f\,,\,\psi\rangle_{L^2(\Gamma)} \quad \text{for all } \psi \in H^{-1/2}(\Gamma). \tag{20}$$

Therefore, also the Lax-Milgram lemma applies and guarantees existence and uniqueness of the solution $\xi \in H^{-1/2}(\Gamma)$. Moreover, the mapping properties (17) imply $\xi \in H^{-1/2+s}(\Gamma)$ provided that $f \in H^{1/2+s}(\Gamma)$ for some $0 \leq s \leq 1/2$.

2.6. Galerkin discretization. Let $\mathcal{T}_\star \in \mathbb{T}$ be a given admissible mesh. Let $T_{\text{ref}} = [0,1]$ for $d = 2$ and $T_{\text{ref}} = \text{conv}\{(0,0),(1,0),(0,1)\}$ for $d = 3$ denote the reference simplices in $\mathbb{R}^{d-1}$. By assumption, each element $T \in \mathcal{T}_\star$ is the image of T_{ref} under an affine bijection $F_T : T_{\text{ref}} \to T$. Let $\mathcal{P}^p(T_{\text{ref}})$ denote the space of all polynomials of degree $\leq p$ on the reference element. Define spaces of $\mathcal{T}_\star$-piecewise polynomials on the boundary Γ by

$$\mathcal{P}^p(\mathcal{T}_\star) := \{\Psi_\star : \Gamma \to \mathbb{R} \,:\, \forall T \in \mathcal{T}_\star \quad \Psi_\star \circ F_T \in \mathcal{P}^p(T_{\text{ref}})\}. \tag{21}$$

Note that $\mathcal{P}^p(\mathcal{T}_\star) \subset L^2(\Gamma) \subset H^{-1/2}(\Gamma)$. Therefore, the Lax-Milgram lemma applies and guarantees existence and uniqueness of the Galerkin approximation $\Xi_\star \in \mathcal{P}^p(\mathcal{T}_\star)$ of ξ which solves

$$\langle\!\langle \Xi_\star\,,\,\Psi_\star \rangle\!\rangle = \langle f\,,\,\Psi_\star\rangle_{L^2(\Gamma)} \quad \text{for all } \Psi_\star \in \mathcal{P}^p(\mathcal{T}_\star). \tag{22}$$

2.7. Weighted-residual error estimator. For any $f \in H^1(\Gamma)$, let $\xi := V^{-1}f$ and $\Xi_\star \in \mathcal{P}^p(\mathcal{T}_\star)$ be its Galerkin approximation (22). Then, for any $\mathcal{R}_\star \subseteq \mathcal{T}_\star$ and any $T \in \mathcal{T}_\star$, the weighted-residual error estimator reads

$$\begin{aligned} \eta_{\xi,\star}(T)^2 &:= |T|^{1/(d-1)} \, \|\nabla(f - V\Xi_\star)\|^2_{L^2(T)}, \\ \eta_{\xi,\star} &:= \eta_{\xi,\star}(\mathcal{T}_\star), \quad \text{where} \quad \eta_{\xi,\star}(\mathcal{R}_\star) := \Big(\sum_{T\in\mathcal{R}_\star} \eta_{\xi,\star}(T)^2 \Big)^{1/2}. \end{aligned} \tag{23}$$

It is well-known [Car97, CMS01] that $\eta_{\xi,\star}$ is reliable $\|\xi - \Xi_\star\|_{H^{-1/2}(\Gamma)} \le C_{\rm rel}\, \eta_{\xi,\star}$, where $C_{\rm rel} > 0$ depends only on Γ as well as γ-shape regularity (8) of $\mathcal{T}_\star$.

3. Adaptive Algorithms and Main Result

The main idea of the following adaptive strategies reads as follows: Let $\phi \in H^{-1/2}(\Gamma)$ be the unique solution of the weakly-singular integral equation (3). For some admissible mesh $\mathcal{T}_\ell \in \mathbb{T}$, let $\Phi_\ell \in \mathcal{P}^p(\mathcal{T}_\ell)$ be the corresponding Galerkin approximation (22) with $f = (K + 1/2)g$. Recall the Galerkin orthogonality

$$\langle V\Psi_\ell \,,\, \phi - \Phi_\ell\rangle_{L^2(\Gamma)} = \langle\!\langle \phi - \Phi_\ell \,,\, \Psi_\ell \rangle\!\rangle = 0 \quad \text{for all } \Psi_\ell \in \mathcal{P}^p(\mathcal{T}_\ell). \tag{24}$$

For fixed $\widetilde{x} \in \Omega$, the fundamental solution $G(\widetilde{x}, \cdot)$ is a smooth function on Γ. With the representation formula (2) and its approximation (4), it thus holds

$$u(\widetilde{x}) - u_\ell(\widetilde{x}) = \widetilde{V}(\phi - \Phi_\ell)(\widetilde{x}) = \langle G(\widetilde{x}, \cdot) \,,\, \phi - \Phi_\ell\rangle_{L^2(\Gamma)} = \langle G(\widetilde{x}, \cdot) - V\Psi_\ell \,,\, \phi - \Phi_\ell\rangle_{L^2(\Gamma)}. \tag{25}$$

Suppose that $\psi = \psi[\widetilde{x}] := V^{-1}G(\widetilde{x}, \cdot)$ and that $\Psi_\ell = \Psi_\ell[\widetilde{x}] \in \mathcal{P}^p(\mathcal{T}_\ell)$ is its Galerkin approximation (22). Then, the latter equality yields

$$\begin{aligned} |u(\widetilde{x}) - u_\ell(\widetilde{x})| &\le \|G(\widetilde{x}, \cdot) - V\Psi_\ell\|_{H^{1/2}(\Gamma)} \, \|\phi - \Phi_\ell\|_{H^{-1/2}(\Gamma)} \\ &\simeq \|\psi[\widetilde{x}] - \Psi_\ell[\widetilde{x}]\|_{H^{-1/2}(\Gamma)} \, \|\phi - \Phi_\ell\|_{H^{-1/2}(\Gamma)}, \end{aligned}$$

where the hidden constants only depend on Γ. Either of these Galerkin errors will be controlled by the respective weighted-residual error estimator which requires additional regularity $g \in H^1(\Gamma)$ for the Dirichlet data. Altogether, we are thus led to

$$|u(\widetilde{x}) - u_\ell(\widetilde{x})| \lesssim \eta_{\phi,\ell}\, \eta_{\psi,\ell}. \tag{26}$$

With these preparations, we consider the following two adaptive algorithms of the form

$$\boxed{\texttt{solve}} \longrightarrow \boxed{\texttt{estimate}} \longrightarrow \boxed{\texttt{mark}} \longrightarrow \boxed{\texttt{refine}},$$

which have been proposed and analyzed by [MS09, BET11] for goal-oriented adaptivity in the context of FEM for the Poisson problem. The first algorithm goes back to [MS09].

Algorithm 1. Input: *Initial mesh $\mathcal{T}_0$, marking parameter $0 < \theta \le 1$, and $C_{\rm mark} \ge 1$.*
Loop: *For all $\ell = 0, 1, 2, 3, \dots$ do* (i)–(viii)*:*

(i) *Compute Galerkin approximation Φ_ℓ to ϕ.*
(ii) *Compute Galerkin approximation $\Psi_\ell[\widetilde{x}]$ to $\psi = \psi[\widetilde{x}]$.*
(iii) *Compute refinement indicators $\eta_{\phi,\ell}(T)$ for all $T \in \mathcal{T}_\ell$.*
(iv) *Compute refinement indicators $\eta_{\psi,\ell}(T)$ for all $T \in \mathcal{T}_\ell$.*
(v) *Determine a set $\mathcal{M}_{\phi,\ell} \subseteq \mathcal{T}_\ell$ of up to the multiplicative factor $C_{\rm mark}$ minimal cardinality such that*

$$\theta\, \eta^2_{\phi,\ell} \le \eta_{\phi,\ell}(\mathcal{M}_{\phi,\ell})^2. \tag{27}$$

(vi) *Determine a set* $\mathcal{M}_{\psi,\ell} \subseteq \mathcal{T}_\ell$ *of up to the multiplicative factor* C_{mark} *minimal cardinality such that*

$$\theta\, \eta_{\psi,\ell}^2 \leq \eta_{\psi,\ell}(\mathcal{M}_{\psi,\ell})^2. \tag{28}$$

(vii) *Choose* $\mathcal{M}_\ell \in \{\mathcal{M}_{\phi,\ell}, \mathcal{M}_{\psi,\ell}\}$ *to be the set of minimal cardinality.*

(viii) *Let* $\mathcal{T}_{\ell+1} := \texttt{refine}(\mathcal{T}_\ell, \mathcal{M}_\ell)$ *be the coarsest refinement of* $\mathcal{T}_\ell$ *such that all marked elements* $T \in \mathcal{M}_\ell$ *have been refined.*

OUTPUT: *Discrete approximations* $\Phi_\ell, \Psi_\ell[\widetilde{x}]$ *and corresponding error estimators* $\eta_{\phi,\ell}, \eta_{\psi,\ell}$ *for all* $\ell \in \mathbb{N}_0$. ■

Remark 2. *For* $C_{\mathrm{mark}} = 1$*, the algorithmic construction of a set* $\mathcal{M}_{\phi,\ell}$ *with minimal cardinality which satisfies, for instance, the Dörfler criterion* (27) *requires sorting of the refinement indicators and thus results in logarithmic-linear complexity. Instead, Stevenson* [Ste07] *proposes an approximate sorting based on binning. This allows the algorithmic construction of some set* $\mathcal{M}_{\phi,\ell}$ *in real linear complexity which satisfies the Dörfler criterion* (27) *and has minimal cardinality up to some multiplicative factor* $C_{\mathrm{mark}} = 2$. ■

The second algorithm has been proposed by [BET11]. Note that both algorithms only differ in the marking strategy: While Algorithm 1 employs a separate Dörfler marking in step (v)–(vii), Algorithm 3 employs a combined Dörfler marking in step (v)–(vi).

Algorithm 3. INPUT:*Initial mesh* $\mathcal{T}_0$*, marking parameter* $0 < \theta \leq 1$*, and* $C_{\mathrm{mark}} \geq 1$.
LOOP: *For all* $\ell = 0, 1, 2, 3, \ldots$ *do* (i)–(vii)*:*

(i) *Compute Galerkin approximation* Φ_ℓ *to* ϕ.

(ii) *Compute Galerkin approximation* $\Psi_\ell[\widetilde{x}]$ *to* $\psi = \psi[\widetilde{x}]$.

(iii) *Compute indicators* $\eta_{\phi,\ell}(T)$ *for all* $T \in \mathcal{T}_\ell$.

(iv) *Compute indicators* $\eta_{\psi,\ell}(T)$ *for all* $T \in \mathcal{T}_\ell$.

(v) *Assemble refinement indicators* $\rho_\ell(T)^2 := \eta_{\phi,\ell}(T)^2\eta_{\psi,\ell}^2 + \eta_{\phi,\ell}^2\eta_{\psi,\ell}(T)^2$ *for all* $T \in \mathcal{T}_\ell$.

(vi) *Determine a set* $\mathcal{M}_\ell \subseteq \mathcal{T}_\ell$ *of up to the multiplicative factor* C_{mark} *minimal cardinality such that*

$$\theta\, \rho_\ell^2 \leq \rho_\ell(\mathcal{M}_\ell)^2, \tag{29}$$

(vii) *Let* $\mathcal{T}_{\ell+1} := \texttt{refine}(\mathcal{T}_\ell, \mathcal{M}_\ell)$ *be the coarsest refinement of* $\mathcal{T}_\ell$ *such that all marked elements* $T \in \mathcal{M}_\ell$ *have been refined.*

OUTPUT: *Discrete approximations* $\Phi_\ell, \Psi_\ell[\widetilde{x}]$ *and corresponding error estimators* $\eta_{\phi,\ell}, \eta_{\psi,\ell}$ *for all* $\ell \in \mathbb{N}_0$. ■

The main result of this work is that Algorithm 1 as well as Algorithm 3 lead to optimal convergence of the product $\eta_{\phi,\ell}\eta_{\psi,\ell}$ of the estimators. To make this precise, we rely on some further notation: Given the initial mesh $\mathcal{T}_0$, let $\mathbb{T}_N := \{\mathcal{T} \in \mathbb{T} : \#\mathcal{T} - \#\mathcal{T}_0 \leq N\}$ denote the (finite) set of all refinements of $\mathcal{T}_0$ which have at most N elements more than $\mathcal{T}_0$. For the statement of the main result, we need the following abstract approximation class for the weighted-residual error estimator $\eta_{\xi,\ell}$. For $s > 0$, we write $\xi \in \mathbb{A}_s$ if

$$\|\xi\|_{\mathbb{A}_s} := \sup_{N\in\mathbb{N}_0} \Big((N+1)^s \min_{\mathcal{T}_\star\in\mathbb{T}_N} \eta_{\xi,\star}\Big) < \infty,$$

where $\eta_{\xi,\star}$ is the weighted-residual error estimator associated with the optimal mesh $\mathcal{T}_\star \in \mathbb{T}_N$. In explicit terms, this means that an algebraic convergence rate $\mathcal{O}(N^{-s})$ for the error estimator is possible, if the optimal meshes are chosen. The following main theorem states that each possible algebraic rate $s > 0$ will asymptotically be realized by the adaptive algorithm.

Theorem 4. *For all $0 < \theta \le 1$, there are constants $0 < q_{\rm lin} < 1$ and $C_{\rm lin} > 0$ such that Algorithm 1 as well as Algorithm 3 are R-linear convergent in the sense of*

$$\eta_{\phi,\ell+n}\eta_{\psi,\ell+n} \le C_{\rm lin} q_{\rm lin}^n \eta_{\phi,\ell}\eta_{\psi,\ell} \quad \text{for all } \ell, n \in \mathbb{N}_0. \tag{30}$$

Moreover, there exist constants $C_{\rm opt}, C_{\rm opt2} > 0$ such that for all $s, t > 0$ and for $0 < \theta \ll 1$ being sufficiently small, $(\phi, \psi[\widetilde{x}]) \in \mathbb{A}_s \times \mathbb{A}_t$ implies

$$\eta_{\phi,\ell}\eta_{\psi,\ell} \le C_{\rm opt} \frac{C_{\rm opt2}^{s+t}}{(1 - q_{\rm lin}^{1/(s+t)})^{s+t}} \|\phi\|_{\mathbb{A}_s} \|\psi[\widetilde{x}]\|_{\mathbb{A}_t} (\#\mathcal{T}_\ell - \#\mathcal{T}_0)^{-(s+t)} \quad \text{for all } \ell \in \mathbb{N}_0, \tag{31}$$

i.e., Algorithm 1 as well as Algorithm 3 guarantee that the product of the error estimators decays with any possible algebraic rate.

Remark 5. *We note that Algorithm 1, Algorithm 3, and Theorem 4 are independent of whether we use direct BEM for the interior problem (based on the Green's formula (2)) or the exterior problem, or indirect BEM, where we solve $V\phi = f$ for some given right-hand side $f \in H^1(\Gamma)$ and aim to approximate $\widetilde{V}\phi(\widetilde{x}) \approx \widetilde{V}\Phi_\ell(\widetilde{x})$ for some $\widetilde{x} \in \mathbb{R}^d \backslash \Gamma$. Moreover, all results hold accordingly if the Dirichlet data g are given, while the hyper singular integral equation is employed to approximate the (unchain) Neumann data.* ■

Remark 6. *Linear convergence (30) is essentially independent of the mesh-refinement used. For $\mathcal{T}_\ell \in \mathbb{T}$ and $\mathcal{T}_\star \in \texttt{refine}(\mathcal{T}_\ell)$, our analysis only requires the following elementary properties:*

- *Each element $T \in \mathcal{T}_\ell$ is the union of its sons, i.e., $T = \bigcup\{T' \in \mathcal{T}_\star : T' \subseteq T\}$.*
- *If $T \in \mathcal{T} \backslash \mathcal{T}_\star$ is refined, its sons $T' \in \mathcal{T}_\star$ with $T' \subseteq T$ satisfy $|T'| \le |T|/2$.*
- *$\mathcal{T}_\star$ is γ-shape regular (8), where γ depends only on $\mathcal{T}_0$.*
- *For $d = 3$, $\mathcal{T}_\star$ is conforming.*

These properties are satisfied for all feasible mesh-refining strategies. However, optimal convergence behavior (31) requires further properties which are satisfied by the mesh-refinement strategies from [AFF+13, KPP13]*; see* (9)–(11). ■

Remark 7. *In principle, our analysis covers goal-oriented adaptivity if the goal function $u(\widetilde{x})$ and its approximation $u_\ell(\widetilde{x})$ satisfy (26), where the error estimators satisfy the properties of Proposition 9 below. For instance, this is the case for goal-oriented FEM for symmetric and elliptic PDEs with L^2-goal functional; see* [CFPP14] *for the verification of the properties* (A1)–(A3) *of Proposition 9. Thus, our analysis also extends the results of* [MS09, BET11] *beyond the Poisson problem to the problem class of* [CKNS08]*. In addition, our analysis avoids any (discrete) efficiency estimates (which are essentially open for BEM) and allows for simple newest vertex bisection, while* [MS09, BET11] *required local bisec5-refinement in the spirit of* [Ste07]*. Details are postponed to a forthcoming work* [FPV14]*, where we shall also address goal-oriented adaptive FEM in case of non-symmetric operators.* ■

Remark 8. *For goal-oriented FEM for the Poisson problem with polynomial data, it is proved in* [BET11] *that Algorithm 3 leads to linear convergence $\texttt{error}_{\ell+1} \le q\,\texttt{error}_\ell$, whereas Algorithm 1 leads only to $\texttt{error}_{\ell+1} \le q^{1/2}\,\texttt{error}_\ell$. Here, $0 < q < 1$, and $\texttt{error}_\star$ is the product of the energy errors with respect to some mesh $\mathcal{T}_\star \in \mathbb{T}$; see* [BET11, eq. (2.12)] *vs.* [BET11, eq. (2.20)]*. Hence, at least in this particular situation, the combined Dörfler marking (29) leads to less adaptive steps and therefore appears to be more effective. Although we did not succeed to prove such a statement in the present case, we shall address this aspect empirically by appropriate numerical experiments in Section 7. Finally, we*

note that our proof of Theorem 4 provides an upper bound $0 < \theta_\star < 1$ *such that optimal convergence rates* (31) *are guaranteed for Algorithm 1 for all* $0 < \theta < \theta_\star$*, but for Algorithm 3 only for all* $0 < \theta < \theta_\star/2$. ■

4. Basic Properties of Weighted-Residual Error Estimator

This section recalls some important properties of the weighted-residual error estimator (23) as well as the elementary consequences for the analysis of Algorihtm 1 and Algorithm 3. Throughout, we use the abbreviate notation $\xi \in \{\phi, \psi[\widetilde{x}]\}$, and $\Xi_\star \in \{\Phi_\star, \Psi_\star[\widetilde{x}]\}$ denotes the respective Galerkin approximation for $\mathcal{T}_\star \in \mathbb{T}$. The following proposition collects some basic properties of the weighted-residual error estimator from the literature (which are called *axioms of adaptivity* in [CFPP14]).

Proposition 9 (basic properties of weighted-residual error estimator)**.** *There are constants* $C_{\rm stb}, C_{\rm red}, C_{\rm rel} > 0$ *and* $0 < q_{\rm red} < 1$ *which depend only on* Γ *and uniform* γ*-shape regularity of the meshes* $\mathcal{T} \in \mathbb{T}$ *such that the following properties* (A1)–(A3) *hold:*

(A1) Stability on non-refined elements*: For each mesh* $\mathcal{T}_\ell \in \mathbb{T}$ *and all refinements* $\mathcal{T}_\star \in \texttt{refine}(\mathcal{T}_\ell)$ *the corresponding error estimators and Galerkin approximations satisfy*

$$\big|\eta_{\xi,\star}(\mathcal{T}_\ell \cap \mathcal{T}_\star) - \eta_{\xi,\ell}(\mathcal{T}_\ell \cap \mathcal{T}_\star)\big| \le C_{\rm stb}\, |\!|\!| \Xi_\ell - \Xi_\star |\!|\!|.$$

(A2) Reduction on refined elements*: For each mesh* $\mathcal{T}_\ell \in \mathbb{T}$ *and all refinements* $\mathcal{T}_\star \in \texttt{refine}(\mathcal{T}_\ell)$ *the corresponding error estimators and Galerkin approximations satisfy*

$$\eta_{\xi,\star}(\mathcal{T}_\star\backslash\mathcal{T}_\ell)^2 \le q_{\rm red}\, \eta_{\xi,\ell}(\mathcal{T}_\ell\backslash\mathcal{T}_\star)^2 + C_{\rm red}\, |\!|\!| \Xi_\ell - \Xi_\star |\!|\!|^2.$$

(A3) Discrete reliability*: For each mesh* $\mathcal{T}_\ell \in \mathbb{T}$ *and all refinements* $\mathcal{T}_\star \in \texttt{refine}(\mathcal{T}_\ell)$*, it holds*

$$|\!|\!| \Xi_\star - \Xi_\ell |\!|\!| \le C_{\rm rel}\, \eta_{\xi,\ell}\big(\mathcal{R}_\xi(\mathcal{T}_\ell, \mathcal{T}_\star)\big),$$

where $\mathcal{R}_\xi(\mathcal{T}_\ell, \mathcal{T}_\star)$ *satisfies* $\mathcal{T}_\ell\backslash\mathcal{T}_\star \subseteq \mathcal{R}_\xi(\mathcal{T}_\ell, \mathcal{T}_\star) \subseteq \mathcal{T}_\ell$ *and* $\#\mathcal{R}_\xi(\mathcal{T}_\ell, \mathcal{T}_\star) \le C_{\rm rel}\, \#(\mathcal{T}_\ell\backslash\mathcal{T}_\star)$ *and hence consists essentially of the refined elements only.*

Sketch of proof. The properties (A1)–(A2) are verified the by inverse-type estimate

$$\|h_\star^{1/2} \nabla_\Gamma V \mathcal{X}_\star\|_{L^2(\Gamma)} \lesssim \|\mathcal{X}_\star\|_{H^{-1/2}(\Gamma)} \quad \text{for all } \mathcal{X}_\star \in \mathcal{P}^p(\mathcal{T}_\star),$$

where the hidden constant depends only on Γ, the shape regularity of the mesh and the polynomial order p. It has first been proved by [FKMP13, Gan13] for lowest-order BEM $p = 0$; see also the more general result [AFF+14] which also applies to curved boundaries. The proofs of (A1) and (A2) are implicitly contained in [FKMP13, Gan13] and also explicitly given in [FFK+14, Proposition 2]. The discrete reliability (A3) is proved in [FKMP13, Gan13] for lowest-order BEM $p = 0$ and in [FFK+14] for general $p \ge 0$. In either case, $\mathcal{R}_\xi(\mathcal{T}_\ell, \mathcal{T}_\star) := \{T \in \mathcal{T}_\ell : \exists T' \in \mathcal{T}_\ell\backslash\mathcal{T}_\star \quad T \cap T' \neq \emptyset\}$ consists of the refined elements $\mathcal{T}_\ell\backslash\mathcal{T}_\star$ plus one additional layer of elements. ■

In the following, we collect some of the results of [CFPP14] as well as some consequences which are required for the analysis of Algorithm 1 and Algorithm 3.

Lemma 10 (discrete reliability implies reliability [CFPP14, Lemma 3.4])**.** *With the constant* $C_{\rm rel} > 0$ *from* (A3)*, it also holds* $|\!|\!| \xi - \Xi_\ell |\!|\!| \le C_{\rm rel}\, \eta_{\xi,\ell}$ *for all* $\mathcal{T}_\ell \in \mathbb{T}$. ■

Lemma 11 (quasi-monotonicity of estimator [CFPP14, Lemma 3.5])**.** *There exists a constant* $C_{\rm mon} > 0$ *which depends only on* (A1)–(A3) *such that for all* $\mathcal{T}_\ell \in \mathbb{T}$ *and all* $\mathcal{T}_\star \in \texttt{refine}(\mathcal{T}_\ell)$*, it holds* $\eta_{\xi,\star}^2 \le C_{\rm mon}\, \eta_{\xi,\ell}^2$. ■

Lemma 12 (optimality of Dörfler marking [CFPP14, Proposition 4.12])**.** *Suppose stability* (A1) *and discrete reliability* (A3)*. For all* $0 < \theta < \theta_\star := (1 + C_{\rm stb}^2 C_{\rm rel}^2)^{-1}$*, there exists some* $0 < \kappa_\star < 1$ *such that for all* $\mathcal{T}_\ell \in \mathbb{T}$ *and all refinements* $\mathcal{T}_\star \in \texttt{refine}(\mathcal{T}_\ell)$ *holds*

$$\eta_{\xi,\star}^2 \le \kappa_\star\, \eta_{\xi,\ell}^2 \quad\Longrightarrow\quad \theta\, \eta_{\xi,\ell}^2 \le \eta_{\xi,\ell}\big(\mathcal{R}_\xi(\mathcal{T}_\ell,\mathcal{T}_\star)\big)^2, \tag{32}$$

where $\mathcal{R}_\xi(\mathcal{T}_\ell,\mathcal{T}_\star)$ *is the set of refined elements from* (A3)*.* ∎

The following contraction result is inspired by [CKNS08, Theorem 4.1].

Lemma 13 (generalized contraction)**.** *Let* $0 < \theta \le 1$*. Let* $\mathcal{T}_\ell \in \mathbb{T}$ *and* $\mathcal{T}_\star \in \texttt{refine}(\mathcal{T}_\ell)$ *be given meshes and suppose that the refined elements satisfy the Dörfler marking, i.e.,*

$$\theta\, \eta_{\xi,\ell}^2 \le \eta_{\xi,\ell}(\mathcal{T}_\ell\backslash\mathcal{T}_\star)^2. \tag{33}$$

Then, there exist constants $0 < q_{\rm conv}, q_{\rm wht} < 1$ *which depend only on* (A1)–(A3) *and* θ*, such that*

$$\Delta_{\xi,\star} \le q_{\rm conv}\, \Delta_{\xi,\ell}, \quad \text{where} \quad \Delta_{\xi,\star} := |\!|\!|\xi - \Xi_\star|\!|\!|^2 + q_{\rm wht}\, \eta_{\xi,\star}^2. \tag{34}$$

Proof. Let $\delta, \varepsilon, q_{\rm wht} > 0$ be constants which are fixed later. The Young inequality $(a+b)^2 \le (1+\delta)a^2 + (1+\delta^{-1})b^2$ and stability (A1) yield

$$\begin{aligned}\eta_{\xi,\star}(\mathcal{T}_\ell \cap \mathcal{T}_\star)^2 &\le (1+\delta)\, \eta_{\xi,\ell}(\mathcal{T}_\ell \cap \mathcal{T}_\star)^2 + C_{\rm stb}^2(1+\delta^{-1})\, |\!|\!|\Xi_\star - \Xi_\ell|\!|\!|^2 \\ &= (1+\delta)\, \eta_{\xi,\ell}^2 - (1+\delta)\, \eta_{\xi,\ell}(\mathcal{T}_\ell\backslash\mathcal{T}_\star)^2 + C_{\rm stb}^2(1+\delta^{-1})\, |\!|\!|\Xi_\star - \Xi_\ell|\!|\!|^2.\end{aligned}$$

Together with reduction (A2), we obtain

$$\begin{aligned}\eta_{\xi,\star}^2 &= \eta_{\xi,\star}(\mathcal{T}_\ell \cap \mathcal{T}_\star)^2 + \eta_{\xi,\star}(\mathcal{T}_\star\backslash\mathcal{T}_\ell)^2 \\ &\le (1+\delta)\, \eta_{\xi,\ell}^2 - (1+\delta-q_{\rm red})\, \eta_{\xi,\ell}(\mathcal{T}_\ell\backslash\mathcal{T}_\star)^2 + \big(C_{\rm stb}^2(1+\delta^{-1}) + C_{\rm red}\big)\, |\!|\!|\Xi_\star - \Xi_\ell|\!|\!|^2.\end{aligned}$$

We note that (20)–(22) give rise to the Galerkin orthogonality

$$\langle\!\langle \xi - \Xi_\star\,,\, Z_\star \rangle\!\rangle = 0 \quad \text{for all } Z_\star \in \mathcal{X}(\mathcal{T}_\star).$$

Together with nestedness $\mathcal{P}^p(\mathcal{T}_\ell) \subseteq \mathcal{P}^p(\mathcal{T}_\star)$, this proves the Pythagorean identity

$$|\!|\!|\xi - \Xi_\star|\!|\!|^2 + |\!|\!|\Xi_\star - \Xi_\ell|\!|\!|^2 = |\!|\!|\xi - \Xi_\ell|\!|\!|^2 \quad \text{for all } \mathcal{T}_\ell \in \mathbb{T} \text{ and } \mathcal{T}_\star \in \texttt{refine}(\mathcal{T}_\ell).$$

With this and $C_\delta := C_{\rm stb}^2(1+\delta^{-1}) + C_{\rm red}$, we thus see

$$\begin{aligned}\Delta_{\xi,\star} &= |\!|\!|\xi - \Xi_\ell|\!|\!|^2 - |\!|\!|\Xi_\star - \Xi_\ell|\!|\!|^2 + q_{\rm wht}\, \eta_{\xi,\star}^2 \\ &\le |\!|\!|\xi - \Xi_\ell|\!|\!|^2 + q_{\rm wht}\big[(1+\delta)\eta_{\xi,\ell}^2 - (1+\delta-q_{\rm red})\, \eta_{\xi,\ell}(\mathcal{T}_\ell\backslash\mathcal{T}_\star)^2\big] + (q_{\rm wht}C_\delta - 1)\, |\!|\!|\Xi_\star - \Xi_\ell|\!|\!|^2 \\ &= \Delta_{\xi,\ell} + q_{\rm wht}\big[\delta\, \eta_{\xi,\ell}^2 - (1+\delta-q_{\rm red})\, \eta_{\xi,\ell}(\mathcal{T}_\ell\backslash\mathcal{T}_\star)^2\big] + (q_{\rm wht}C_\delta - 1)\, |\!|\!|\Xi_\star - \Xi_\ell|\!|\!|^2. \\ &\overset{(33)}{\le} \Delta_{\xi,\ell} + q_{\rm wht}\, \eta_{\xi,\ell}^2\big[\delta - (1+\delta-q_{\rm red})\, \theta\big] + (q_{\rm wht}C_\delta - 1)\, |\!|\!|\Xi_\star - \Xi_\ell|\!|\!|^2.\end{aligned}$$

Choose $0 < \delta \ll 1$ such that $-\varepsilon := \delta - (1+\delta-q_{\rm red})\,\theta < 0$. Choose $0 < q_{\rm wht} \ll 1$ such that $q_{\rm wht}C_\delta \le 1$. Reliability $|\!|\!|\xi - \Xi_\ell|\!|\!| \le C_{\rm rel}\eta_{\xi,\ell}$ gives $\Delta_{\xi,\ell} \le (C_{\rm rel}^2 + q_{\rm wht})\, \eta_{\xi,\ell}^2$ and hence results in

$$\Delta_{\xi,\star} \le \Delta_{\xi,\ell} - \varepsilon q_{\rm wht}\, \eta_{\xi,\ell}^2 \le \Big(1 - \frac{\varepsilon q_{\rm wht}}{C_{\rm rel}^2 + q_{\rm wht}}\Big)\, \Delta_{\xi,\ell} =: q_{\rm conv}\, \Delta_{\xi,\ell}.$$

This concludes the proof. ∎

Proposition 14 (generalized R-linear convergence)**.** *Let $\mathcal{T}_\ell$ be a sequence of successively refined meshes, i.e., $\mathcal{T}_\ell \in \texttt{refine}(\mathcal{T}_{\ell-1})$ for all $\ell \in \mathbb{N}$. Let $0 < \theta \le 1$. Then, there are constants $0 < q_{\rm conv} < 1$ and $C_{\rm conv} > 0$ which depend only on* (A1)–(A3) *and θ, such that the following holds: Let $\ell, n \in \mathbb{N}_0$ and suppose that there are at least $k \le n$ indices $\ell \le j_1 < j_2 < \cdots < j_k < \ell + n$ such that the Dörfer marking* (33) *is satisfied on the refined elements, i.e.,*

$$\theta\, \eta_{\xi,j_m}^2 \le \eta_{\xi,j_m}(\mathcal{T}_{j_m}\backslash\mathcal{T}_{j_m+1})^2 \quad \text{for all } m = 1, \dots k. \tag{35}$$

Then, the error estimator satisfies

$$\eta_{\xi,\ell+n}^2 \le C_{\rm conv}\, q_{\rm conv}^k\, \eta_{\xi,\ell}^2. \tag{36}$$

Proof. Recall the definition (34) of the quantities $\Delta_{\xi,\star}$ from Lemma 13 and note that

$$q_{\rm wht}\, \eta_{\xi,\ell}^2 \le \Delta_{\xi,\ell} \quad \text{and} \quad \Delta_{\xi,\star} \le (C_{\rm rel}^2 + q_{\rm wht})\, \eta_{\xi,\star}^2.$$

With Lemma 11 and $C'_{\rm mon} = (C_{\rm rel}^2 + q_{\rm wht}) C_{\rm mon} q_{\rm wht}^{-1}$, we thus see quasi-monotonicity $\Delta_{\xi,\star} \le C'_{\rm mon}\, \Delta_{\xi,\ell}$ for all $\mathcal{T}_\star \in \texttt{refine}(\mathcal{T}_\ell)$. Iterative application of Lemma 13 yields

$$\begin{aligned} q_{\rm wht}\, \eta_{\xi,\ell+n}^2 \le \Delta_{\xi,\ell+n} \le q_{\rm conv}\, \Delta_{\xi,j_k} \le q_{\rm conv}^2\, \Delta_{\xi,j_{k-1}} \le \cdots \le q_{\rm conv}^k\, \Delta_{\xi,j_1} &\le q_{\rm conv}^k\, C'_{\rm mon}\, \Delta_{\xi,\ell} \\ &\le q_{\rm conv}^k\, C'_{\rm mon} (C_{\rm rel}^2 + q_{\rm wht})\, \eta_{\xi,\ell}^2 \end{aligned}$$

This concludes $C_{\rm conv} = q_{\rm wht}^{-1} C'_{\rm mon}(C_{\rm rel}^2 + q_{\rm wht}) = (C_{\rm rel}^2 + q_{\rm wht})^2 C_{\rm mon} q_{\rm wht}^{-2}$. ∎

5. Proof of Theorem 4 for Algorithm 1

Recall that the error estimators $\eta_{\phi,\ell}$ and $\eta_{\psi,\ell}$ satisfy the properties (A1)–(A3) of Proposition 9. Throughout this section and for the ease of presentation, we suppose, without loss of generality, that $\eta_{\phi,\ell}$ and $\eta_{\psi,\ell}$ satisfy (A1)–(A3) even with the same constants.

Proof of linear convergence* (30) *of Algorithm 1. In each step of Algorithm 1, the set $\mathcal{M}_\ell$ satisfies either the Dörfler marking (27) for $\eta_{\phi,\ell}$ or (28) for $\eta_{\psi,\ell}$. With $\mathcal{M}_\ell \subseteq \mathcal{T}_\ell\backslash\mathcal{T}_{\ell+1}$, this implies that within n successive steps $j = \ell, \dots, \ell+n$ of the adaptive algorithm, $\mathcal{T}_j\backslash\mathcal{T}_{j+1}$ satisfies k-times the Dörfler marking for $\eta_{\phi,\ell}$ and $(n-k)$-times the Dörfler marking for $\eta_{\psi,\ell}$. According to Proposition 14, this implies

$$\eta_{\phi,\ell+n}^2 \le C_{\rm conv}\, q_{\rm conv}^k\, \eta_{\phi,\ell}^2 \quad \text{as well as} \quad \eta_{\psi,\ell+n}^2 \le C_{\rm conv}\, q_{\rm conv}^{n-k}\, \eta_{\psi,\ell}^2.$$

Altogether, this proves

$$\eta_{\phi,\ell+n}^2\, \eta_{\psi,\ell+n}^2 \le C_{\rm conv}^2\, q_{\rm conv}^n\, \eta_{\phi,\ell}^2\, \eta_{\psi,\ell}^2.$$

This concludes (30) with $q_{\rm lin} = q_{\rm conv}^{1/2}$ and $C_{\rm lin} = C_{\rm conv}$. ∎

Unlike linear convergence, the proof of optimal convergence rates is more tailored to the mesh-refinement used. The heart of the matter of the following optimality analysis is to find an appropriate refinement $\mathcal{T}_\star \in \texttt{refine}(\mathcal{T}_\ell)$.

Claim 5.1. *There exists a constant $C_1 > 0$ such that, given $0 < \kappa < 1$, each mesh $\mathcal{T}_\ell \in \mathbb{T}$ admits some refinement $\mathcal{T}_\star \in \texttt{refine}(\mathcal{T}_\ell)$ such that for all $s, t > 0$ with $(\phi, \psi[\widetilde{x}]) \in \mathbb{A}_s \times \mathbb{A}_t$ holds*

$$\#\mathcal{T}_\star - \#\mathcal{T}_\ell \le 2\, (C_1 \kappa^{-1/2}\, \|\phi\|_{\mathbb{A}_s} \|\psi[\widetilde{x}]\|_{\mathbb{A}_t})^{1/(s+t)}\, (\eta_{\phi,\ell}\eta_{\psi,\ell})^{-1/(s+t)}, \tag{37}$$

$$\eta_{\phi,\star}^2 \eta_{\psi,\star}^2 \le \kappa\, \eta_{\phi,\ell}^2 \eta_{\psi,\ell}^2. \tag{38}$$

Proof. Define $\varepsilon := C_{\mathrm{mon}}^{-1}\kappa^{1/2}\,\eta_{\phi,\ell}\eta_{\psi,\ell}$. Note that $\varepsilon \le \kappa^{1/2}\,\eta_{\phi,0}\eta_{\psi,0} < \|\phi\|_{\mathbb{A}_s}\|\psi[\widetilde{x}]\|_{\mathbb{A}_t} < \infty$. Choose the minimal $N \in \mathbb{N}_0$ with $\|\phi\|_{\mathbb{A}_s}\|\psi[\widetilde{x}]\|_{\mathbb{A}_t} \le \varepsilon\,(N+1)^{s+t}$. By minimality, it holds

$$N < (\|\phi\|_{\mathbb{A}_s}\|\psi[\widetilde{x}]\|_{\mathbb{A}_t})^{1/(s+t)}\varepsilon^{-1/(s+t)} = C\,(\eta_{\phi,\ell}\eta_{\psi,\ell})^{-1/(s+t)}$$

with $C := (\|\phi\|_{\mathbb{A}_s}\|\psi[\widetilde{x}]\|_{\mathbb{A}_t})^{1/(s+t)}(C_{\mathrm{mon}}^{-1}\kappa^{1/2})^{-1/(s+t)} = (C_{\mathrm{mon}}\kappa^{-1/2}\,\|\phi\|_{\mathbb{A}_s}\|\psi[\widetilde{x}]\|_{\mathbb{A}_t})^{1/(s+t)}$. Choose $\mathcal{T}_{\varepsilon_1}, \mathcal{T}_{\varepsilon_2} \in \mathbb{T}_N$ with $\eta_{\phi,\varepsilon_1} = \min_{\mathcal{T}_\star\in\mathbb{T}_N}\eta_{\phi,\star}$ and $\eta_{\psi,\varepsilon_2} = \min_{\mathcal{T}_\star\in\mathbb{T}_N}\eta_{\psi,\star}$. Define $\mathcal{T}_\varepsilon := \mathcal{T}_{\varepsilon_1}\oplus\mathcal{T}_{\varepsilon_2}$ and $\mathcal{T}_\star := \mathcal{T}_\varepsilon\oplus\mathcal{T}_\ell$. The overlay estimate (10) yields

$$\#\mathcal{T}_\star - \#\mathcal{T}_\ell \le \#\mathcal{T}_\varepsilon - \#\mathcal{T}_0 \le \#\mathcal{T}_{\varepsilon_1} + \#\mathcal{T}_{\varepsilon_2} - 2\,\#\mathcal{T}_0 \le 2N < 2C\,(\eta_{\phi,\ell}\eta_{\psi,\ell})^{-1/(s+t)}.$$

Moreover, quasi-monotonicity of the estimators (Lemma 11), the definition of the approximation classes, and the choice of N give

$$\eta_{\phi,\star}\eta_{\psi,\star} \le C_{\mathrm{mon}}\eta_{\phi,\varepsilon_1}\eta_{\psi,\varepsilon_2} \le C_{\mathrm{mon}}(N+1)^{-(s+t)}\|\phi\|_{\mathbb{A}_s}\|\psi[\widetilde{x}]\|_{\mathbb{A}_t} \le C_{\mathrm{mon}}\varepsilon = \kappa^{1/2}\,\eta_{\phi,\ell}\eta_{\psi,\ell}.$$

This concludes the proof with $C_1 = C_{\mathrm{mon}}$. ∎

Claim 5.2. *Suppose that $0 < \theta < \theta_\star := (1 + C_{\mathrm{stb}}^2 C_{\mathrm{rel}}^2)^{-1}$. Then, there exist constants $C_2, C_3 > 0$ such that for all $s, t > 0$ with $(\phi, \psi[\widetilde{x}]) \in \mathbb{A}_s \times \mathbb{A}_t$, the set of marked elements $\mathcal{M}_\ell$ of Algorithm 1 satisfies*

$$\#\mathcal{M}_\ell \le C_2\,(C_3\|\phi\|_{\mathbb{A}_s}\|\psi[\widetilde{x}]\|_{\mathbb{A}_t})^{1/(s+t)}\,(\eta_{\phi,\ell}\eta_{\psi,\ell})^{-1/(s+t)}$$

Proof. Adopt the notation of Lemma 12. Choose $\kappa = \kappa_\star^2$ in Claim 5.1. Then, the constructed mesh $\mathcal{T}_\star \in \mathtt{refine}(\mathcal{T}_\ell)$ satisfies $\eta_{\phi,\star}^2\eta_{\psi,\star}^2 \le \kappa_\star^2\,\eta_{\phi,\ell}^2\eta_{\psi,\ell}^2$. This implies $\eta_{\phi,\star}^2 \le \kappa_\star\,\eta_{\phi,\ell}^2$ or $\eta_{\psi,\star}^2 \le \kappa_\star\,\eta_{\psi,\ell}^2$ and hence the Dörfler marking with $\eta_{\phi,\ell}$ and $\mathcal{R}_\phi(\mathcal{T}_\ell, \mathcal{T}_\star)$ or with $\eta_{\psi,\ell}$ and $\mathcal{R}_\psi(\mathcal{T}_\ell, \mathcal{T}_\star)$. In any case, this implies

$$\begin{aligned}\#\mathcal{M}_\ell = \min\{\#\mathcal{M}_{\phi,\ell}\,,\,\#\mathcal{M}_{\psi,\ell}\} &\le C_{\mathrm{mark}}\,\min\{\#\mathcal{R}_\phi(\mathcal{T}_\ell,\mathcal{T}_\star)\,,\,\#\mathcal{R}_\psi(\mathcal{T}_\ell,\mathcal{T}_\star)\}\\ &\le C_{\mathrm{mark}}C_{\mathrm{rel}}\,\#(\mathcal{T}_\ell\backslash\mathcal{T}_\star).\end{aligned}$$

Since bisection guarantees that refined elements are refined into at least two sons, it holds

$$\#(\mathcal{T}_\ell\backslash\mathcal{T}_\star) \le \#\mathcal{T}_\star - \#\mathcal{T}_\ell \le 2\,(C_1\kappa_\star^{-1}\|\phi\|_{\mathbb{A}_s}\|\psi[\widetilde{x}]\|_{\mathbb{A}_t})^{1/(s+t)}\,(\eta_{\phi,\ell}\eta_{\psi,\ell})^{-1/(s+t)}.$$

This concludes the proof with $C_2 = 2C_{\mathrm{mark}}C_{\mathrm{rel}}$ and $C_3 = C_1\kappa_\star^{-1}$. ∎

Proof of optimal convergence* (31) *of Algorithm 1. With the mesh-closure estimate (11) and Claim 5.2, we obtain

$$\#\mathcal{T}_\ell - \#\mathcal{T}_0 \le C_{\mathrm{mesh}}\sum_{j=0}^{\ell-1}\#\mathcal{M}_j \le C_{\mathrm{mesh}}C_2\,(C_3\|\phi\|_{\mathbb{A}_s}\|\psi[\widetilde{x}]\|_{\mathbb{A}_t})^{1/(s+t)}\sum_{j=0}^{\ell-1}(\eta_{\phi,j}\eta_{\psi,j})^{-1/(s+t)}.$$

R-linear convergence (30) implies

$$\eta_{\phi,\ell}\eta_{\psi,\ell} \le C_{\mathrm{lin}}\,q_{\mathrm{lin}}^{\ell-j}\eta_{\phi,j}\eta_{\psi,j} \quad \text{for all } 0 \le j \le \ell$$

and hence

$$(\eta_{\phi,j}\eta_{\psi,j})^{-1/(s+t)} \le C_{\mathrm{lin}}^{1/(s+t)}q_{\mathrm{lin}}^{(\ell-j)/(s+t)}(\eta_{\phi,\ell}\eta_{\psi,\ell})^{-1/(s+t)}.$$

With $0 < q := q_{\mathrm{lin}}^{1/(s+t)} < 1$, the geometric series applies and yields

$$\sum_{j=0}^{\ell-1}(\eta_{\phi,j}\eta_{\psi,j})^{-1/(s+t)} \le C_{\mathrm{lin}}^{1/(s+t)}(\eta_{\phi,\ell}\eta_{\psi,\ell})^{-1/(s+t)}\sum_{j=0}^{\ell-1}q^{\ell-j} \le \frac{C_{\mathrm{lin}}^{1/(s+t)}}{1-q_{\mathrm{lin}}^{1/(s+t)}}\,(\eta_{\phi,\ell}\eta_{\psi,\ell})^{-1/(s+t)}.$$

Combining this with the first estimate, we obtain

$$\#\mathcal{T}_\ell - \#\mathcal{T}_0 \le \frac{C_{\mathrm{mesh}}C_2}{1-q_{\mathrm{lin}}^{1/(s+t)}} \left(C_{\mathrm{lin}}C_3\,\|\phi\|_{\mathbb{A}_s}\|\psi[\widetilde{x}]\|_{\mathbb{A}_t}\right)^{1/(s+t)} (\eta_{\phi,\ell}\eta_{\psi,\ell})^{-1/(s+t)}.$$

Rearranging this estimate, we conclude (31) with $C_{\mathrm{opt}} = C_{\mathrm{lin}}C_3$ and $C_{\mathrm{opt2}} = C_{\mathrm{mesh}}C_2$. ■

6. Proof of Theorem 4 for Algorithm 3

As in the previous section, we suppose that $\eta_{\phi,\ell}$ and $\eta_{\psi,\ell}$ satisfy the properties (A1)–(A3) of Proposition 9 even with the same constants.

Proof of linear convergence* (30) *of Algorithm 3. Note that $\rho_\ell^2 = 2\,\eta_{\phi,\ell}^2\eta_{\psi,\ell}^2$. Therefore, (29) becomes

$$2\theta\,\eta_{\phi,\ell}^2\eta_{\psi,\ell}^2 \le \eta_{\phi,\ell}(\mathcal{M}_\ell)^2\,\eta_{\psi,\ell}^2 + \eta_{\phi,\ell}^2\,\eta_{\psi,\ell}(\mathcal{M}_\ell)^2.$$

In particular, this shows that

$$\theta\,\eta_{\phi,\ell}^2 \le \eta_{\phi,\ell}(\mathcal{M}_\ell)^2 \quad \text{or} \quad \theta\,\eta_{\psi,\ell}^2 \le \eta_{\psi,\ell}(\mathcal{M}_\ell)^2.$$

In the proof of Theorem 4 for Algorithm 1, we have seen that this already ensures linear convergence (30) with $q_{\mathrm{lin}} = q_{\mathrm{conv}}^{1/2}$. ■

The proof of optimal convergence (31) for Algorithm 3 is essentially a consequence of the following elementary observation.

Claim 6.1. *Let $0 < \theta \le 1/2$. Suppose that $\mathcal{R}_\ell \subseteq \mathcal{T}_\ell$ satisfies*

$$2\theta\,\eta_{\phi,\ell}^2 \le \eta_{\phi,\ell}(\mathcal{R}_\ell)^2 \quad \textit{or} \quad 2\theta\,\eta_{\psi,\ell}^2 \le \eta_{\psi,\ell}(\mathcal{R}_\ell)^2.$$

Then, by definition of ρ_ℓ in step (iii) *of Algorithm 3, it follows*

$$\theta\,\rho_\ell^2 \le \rho_\ell(\mathcal{R}_\ell)^2. \tag{39}$$

Proof. It holds $\theta\,\rho_\ell^2 = 2\theta\,\eta_{\phi,\ell}^2\eta_{\psi,\ell}^2 \le \eta_{\phi,\ell}(\mathcal{R}_\ell)^2\,\eta_{\psi,\ell}^2 + \eta_{\phi,\ell}^2\,\eta_{\psi,\ell}(\mathcal{R}_\ell)^2 = \rho_\ell(\mathcal{R}_\ell)^2$. ■

With this observation, Claim 5.2 of the proof of Estimate (31) holds accordingly. Our proof yields that the upper bound $\theta_\star$ for optimal marking parameters in Algorithm 3 is half that for optimal marking parameters in Algorithm 1.

Claim 6.2. *Suppose that $0 < \theta < \theta_\star/2$ with $\theta_\star := (1 + C_{\mathrm{stb}}^2C_{\mathrm{rel}}^2)^{-1}$. Then, there exist constants $C_2, C_3 > 0$ such that for all $s,t > 0$ with $(\phi,\psi[\widetilde{x}]) \in \mathbb{A}_s \times \mathbb{A}_t$, the set of marked elements $\mathcal{M}_\ell$ of Algorithm 3 satisfies*

$$\#\mathcal{M}_\ell \le C_2\left(C_3\|\phi\|_{\mathbb{A}_s}\|\psi[\widetilde{x}]\|_{\mathbb{A}_t}\right)^{1/(s+t)} (\eta_{\phi,\ell}\eta_{\psi,\ell})^{-1/(s+t)}$$

Proof. We first note that Claim 5.1 is not affected by the marking strategy and hence applies to the present setting as well. We proceed as in the proof of Claim 5.2: Adopt the notation of Lemma 12. Choose $\kappa = \kappa_\star^2$ in Claim 5.1. Then, the constructed mesh $\mathcal{T}_\star \in \mathtt{refine}(\mathcal{T}_\ell)$ satisfies $\eta_{\phi,\star}^2\eta_{\psi,\star}^2 \le \kappa_\star^2\,\eta_{\phi,\ell}^2\eta_{\psi,\ell}^2$. This implies $\eta_{\phi,\star}^2 \le \kappa_\star\,\eta_{\phi,\ell}^2$ or $\eta_{\psi,\star}^2 \le \kappa_\star\,\eta_{\psi,\ell}^2$. Hence, the Dörfler marking with marking parameter 2θ holds for $\eta_{\phi,\ell}$ and $\mathcal{R}_\phi(\mathcal{T}_\ell,\mathcal{T}_\star)$ or for $\eta_{\psi,\ell}$ and $\mathcal{R}_\psi(\mathcal{T}_\ell,\mathcal{T}_\star)$. According to Claim 6.1, the Dörfler marking (39) with marking parameter θ holds for ρ_ℓ and $\mathcal{R}_\phi(\mathcal{T}_\ell,\mathcal{T}_\star)$ or $\mathcal{R}_\psi(\mathcal{T}_\ell,\mathcal{T}_\star)$. In any case, this implies

$$\#\mathcal{M}_\ell \le C_{\mathrm{mark}}\,\max\{\#\mathcal{R}_\phi(\mathcal{T}_\ell,\mathcal{T}_\star)\,,\,\#\mathcal{R}_\psi(\mathcal{T}_\ell,\mathcal{T}_\star)\} \le C_{\mathrm{mark}}C_{\mathrm{rel}}\,\#(\mathcal{T}_\ell\backslash\mathcal{T}_\star).$$

Since bisection guarantees that refined elements are refined into at least two sons, it holds

$$\#(\mathcal{T}_\ell\backslash\mathcal{T}_\star) \le \#\mathcal{T}_\star - \#\mathcal{T}_\ell \le 2\left(C_1\kappa_\star^{-1}\|\phi\|_{\mathbb{A}_s}\|\psi[\widetilde{x}]\|_{\mathbb{A}_t}\right)^{1/(s+t)} (\eta_{\phi,\ell}\eta_{\psi,\ell})^{-1/(s+t)}.$$

This concludes the proof with $C_2 = 2C_{\mathrm{mark}}C_{\mathrm{rel}}$ and $C_3 = C_1\kappa_\star^{-1}$. ■

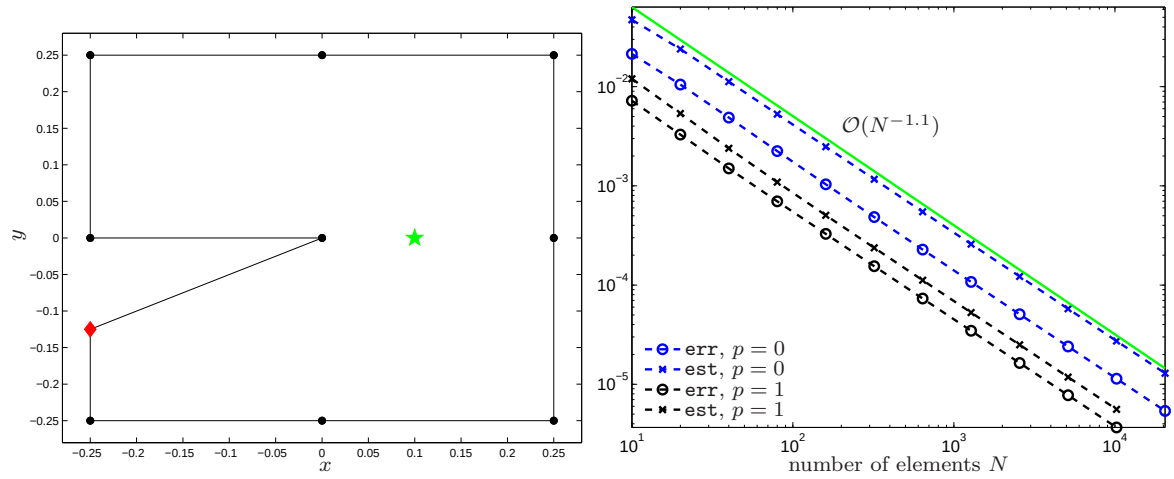

FIGURE 1. Example 7.1: Geometry and initial partition (left), where the red node (diamond) is given by $(-0.25, -0.125)$ and the green star indicates the evaluation point $\widetilde{x} = (0.1, 0)$. Uniform mesh-refinement leads to a reduced convergence order for $p = 0, 1$ (right).

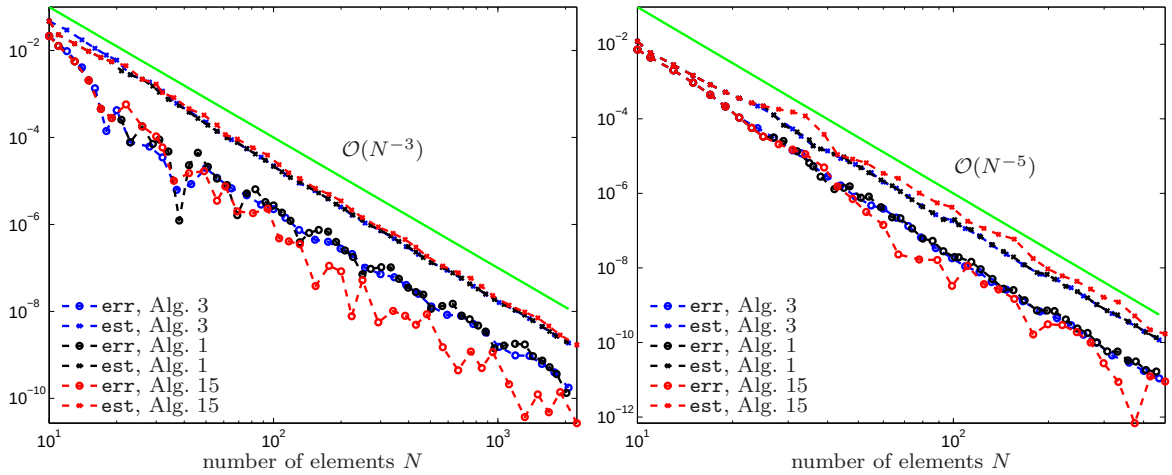

FIGURE 2. Example 7.1: Experimental convergence of adaptive algorithms with $\theta = 0.4$ for $p = 0$ (left) and $p = 1$ (right), where the respective green line indicates the optimal rate of convergence $\mathcal{O}(N^{-(2p+3)})$.

Proof of optimal convergence* (31) *of Algorithm 3. The proof follows verbatim to the proof of the corresponding estimate for Algorithm 1, since that proof essentially relies only on the validity of Claim 5.2 which is replaced by Claim 6.2. ■

7. EXPERIMENTS

In this section, we compare different adaptive strategies with respect to convergence of point errors as well as the estimator product

$$\texttt{err}_\ell(\widetilde{x}) := |u(\widetilde{x}) - u_\ell(\widetilde{x})| \lesssim \eta_{\phi,\ell}\eta_{\psi,\ell} =: \texttt{est}_\ell(\widetilde{x}). \tag{40}$$

Here, $u(\widetilde{x})$ is the point value for the exact solution $u \in C^\infty(\Omega) \cap H^1(\Omega)$ of (1) and $u_\ell(\widetilde{x})$ is defined through the representation formula (4). Recall that $\widetilde{x}$-dependence of the

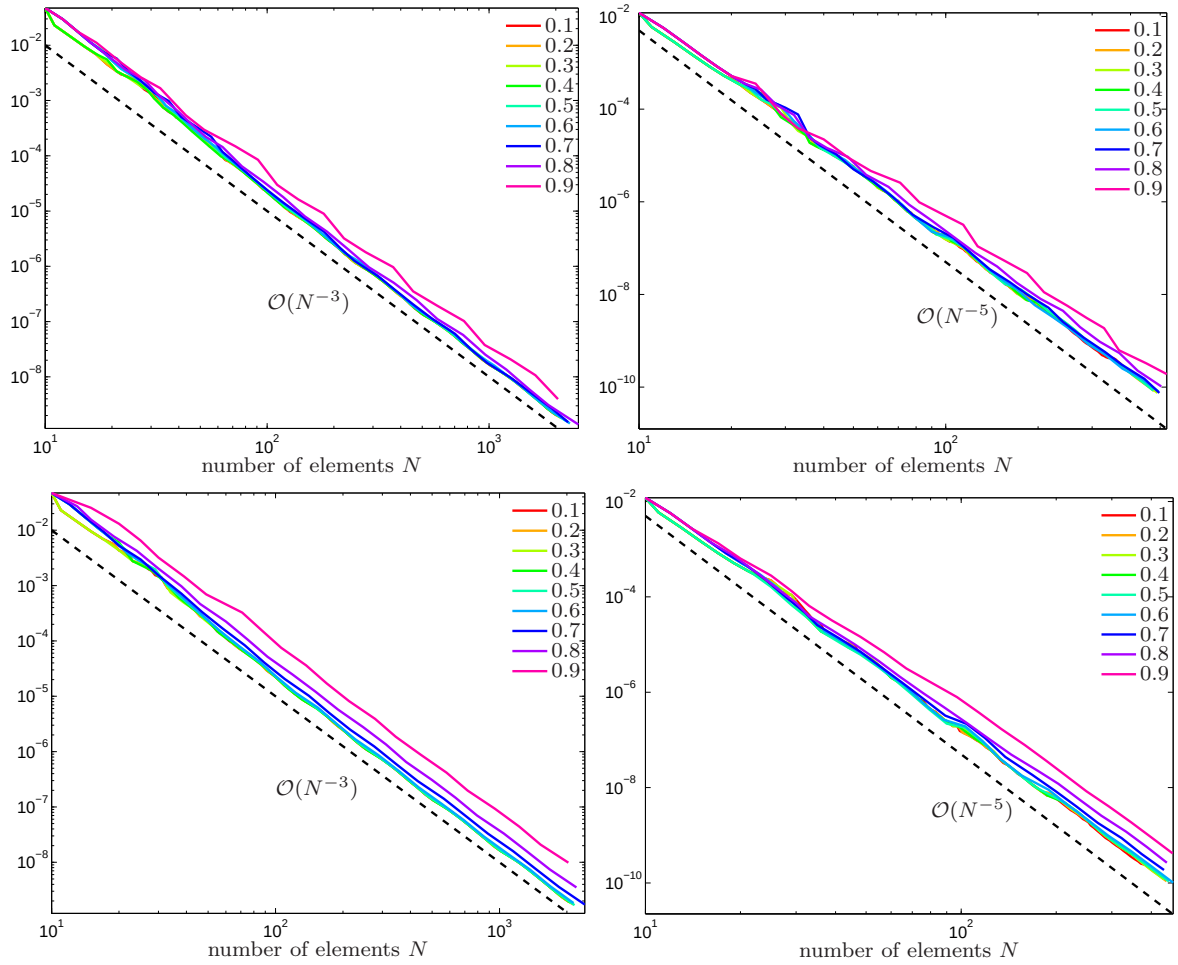

FIGURE 3. Example 7.1: Experimental convergence behavior of Algorithm 1 (top) and Algorithm 3 (bottom) for the estimator product $\mathtt{est}_\ell(\widetilde{x})$ and different parameters $\theta \in \{0.1, \dots, 0.9\}$: $p = 0$ (left) vs. $p = 1$ (right).

estimator product stems from $\psi = \psi[\widetilde{x}] := V^{-1}G(\widetilde{x}, \cdot)$. We shall write $\mathtt{err}_\ell = \mathtt{err}_\ell(\widetilde{x})$ and $\mathtt{est}_\ell = \mathtt{est}_\ell(\widetilde{x})$ if the evaluation point $\widetilde{x}$ is clear from the context.

Besides the adaptive strategies from Algorithm 1 and Algorithm 3, we consider the following usual adaptive algorithm for the energy error. Note that this is also formally obtained by replacing step (vii) of Algorithm 1 by the definition $\mathcal{M}_\ell := \mathcal{M}_{\phi,\ell}$. It is known [FKMP13, Gan13, FFK+14, FFK+13] that this algorithm leads to linear convergence with optimal rates for $\eta_{\phi,\ell}$. For either algorithm (Algorithm 1, 3, 15), we use $C_{\mathrm{mark}} = 1$ and compare the performance with respect to $\mathtt{est}_\ell(\widetilde{x})$ and $\mathtt{err}_\ell(\widetilde{x})$.

Algorithm 15. INPUT: *Initial mesh $\mathcal{T}_0$, marking parameter $0 < \theta \le 1$, and $C_{\mathrm{mark}} \ge 1$.*
LOOP: *For all $\ell = 0, 1, 2, 3, \dots$ do* (i)–(iv)*:*

(i) *Compute Galerkin approximation Φ_ℓ to ϕ.*
(ii) *Compute refinement indicators $\eta_{\phi,\ell}(T)$ for all $T \in \mathcal{T}_\ell$.*
(iii) *Determine a set $\mathcal{M}_\ell \subseteq \mathcal{T}_\ell$ of up to the multiplicative factor C_{mark} minimal cardinality such that*

$$\theta\, \eta_{\phi,\ell}^2 \le \eta_{\phi,\ell}(\mathcal{M}_\ell)^2. \tag{41}$$

(iv) *Let $\mathcal{T}_{\ell+1} := \mathtt{refine}(\mathcal{T}_\ell, \mathcal{M}_\ell)$ be the coarsest refinement of $\mathcal{T}_\ell$ such that all marked elements $T \in \mathcal{M}_\ell$ have been refined.*

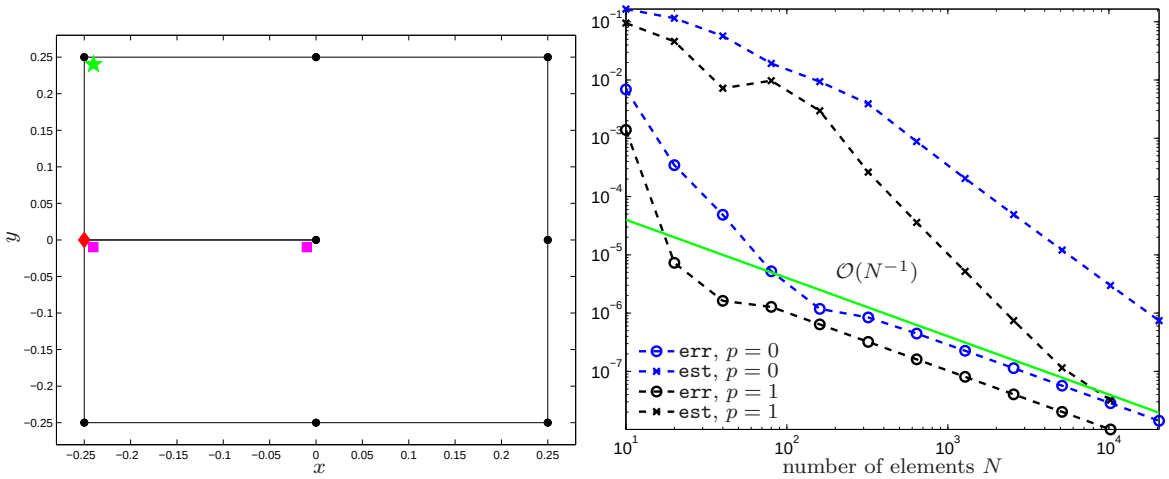

FIGURE 4. Example 7.2: Geometry and initial partition (left), where the red node (diamond) is given by $(-0.25, -0.0001)$ and the green dot indicates the evaluation point $\widetilde{x} = (-0.24, 0.24)$. The magenta squares indicate additional evaluation points, which are not used for steering the adaptive algorithms (left). Uniform mesh-refinement leads to a reduced convergence order of approximately $\mathcal{O}(N^{-1})$ for $p = 0, 1$ (right).

OUTPUT: *Discrete approximations* Φ_ℓ *and corresponding error estimators* $\eta_{\phi,\ell}$ *for all* $\ell \in \mathbb{N}_0$. ■

For 2D, we consider two geometries with reentrant corner visualized in Figure 1 resp. Figure 4. For 3D, we consider the U-domain from Figure 9 with two reentrant edges. In each experiment, we prescribe an exact solution with generic singularity at the reentrant corner/edge and observe that therefore point errors $\texttt{err}_\ell(\widetilde{x})$ as well the upper bound $\texttt{est}_\ell(\widetilde{x})$ show reduced orders of convergence for uniform mesh-refinement. The 2D experiments are performed with the MATLAB library `HILBERT` [AEF+14], while we rely on an own extension of the C++ library `BEM++` [SAB+14] for the 3D experiments.

Example 7.1. Z-shaped domain in 2D. We consider the domain $\Omega \subset \mathbb{R}^2$ shown in Figure 1. There, the node indicated by the red diamond, is $(-0.25, -d)$ with $d = 0.125$. We prescribe the exact solution of (1) in 2D polar coordinates (r, φ) by

$$u(x,y) = r^{\pi/\alpha} \cos\left(\frac{\pi}{\alpha}\varphi\right) \quad \text{with} \quad \alpha = 2\pi - \arcsin\left(d/\sqrt{(\tfrac{1}{4})^2 + d^2}\right), \tag{42}$$

where α is the (interior) angle at the reentrant corner $(0,0)$. We note that u as well as its normal derivative $\phi = \partial_n u$ have generic singularities at $(0,0)$. This is reflected by a reduced order of convergence $\mathcal{O}(N^{-1.1})$ for the point error $\texttt{err}_\ell(\widetilde{x})$ as well as the estimator product $\texttt{est}_\ell(\widetilde{x})$ from (40) for both, piecewise constant ($p = 0$) as well as piecewise linear ($p = 1$) BEM discretizations; see Figure 1.

Adaptivity by either algorithm (Algorithm 1, 3, 15) leads to optimal convergence behavior; see Figure 2 for $p \in \{0, 1\}$ and $\theta = 0.4$. Other choices of, e.g., $\theta \in \{0.1, 0.2\}$ lead to similar results (not displayed). For Algorithm 1 and Algorithm 3, we study the dependence of optimal convergence rates on the choice of the marking parameter $\theta \in \{0.1, \dots, 0.9\}$ in Figure 3 for the estimator product $\texttt{est}_\ell(\widetilde{x})$. Essentially, each choice of θ leads to optimal convergence. The same is observed for the point error $\texttt{err}_\ell(\widetilde{x})$ (not displayed).

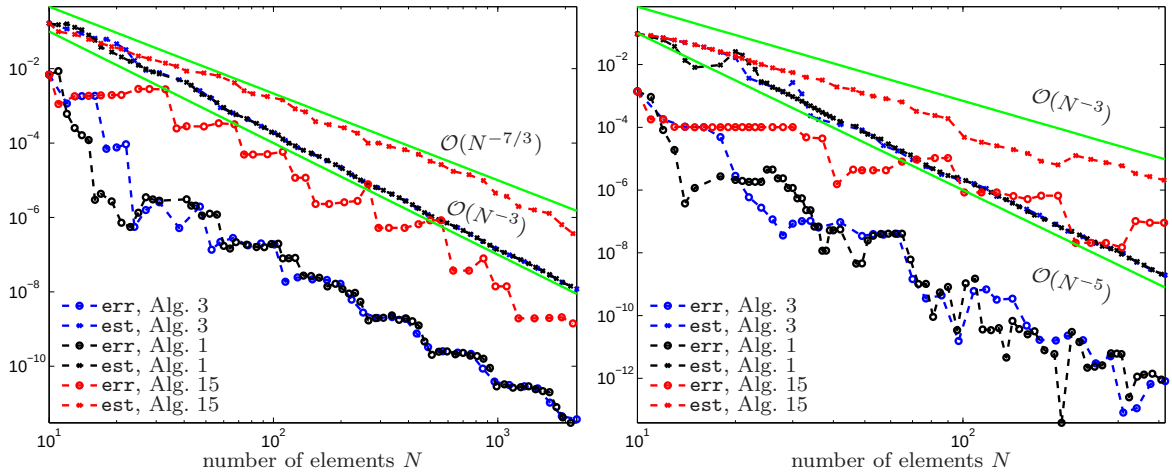

FIGURE 5. Example 7.2: Experimental convergence of adaptive algorithms with $\theta = 0.4$ for $p = 0$ (left) and $p = 1$ (right). The respective green lines indicate the optimal rate of convergence $\mathcal{O}(N^{-(2p+3)})$ as well as worse orders of convergence $\mathcal{O}(N^{-(2+1/3)})$ (left) resp. $\mathcal{O}(N^{-3})$ (right) which are observed for Algorithm 15.

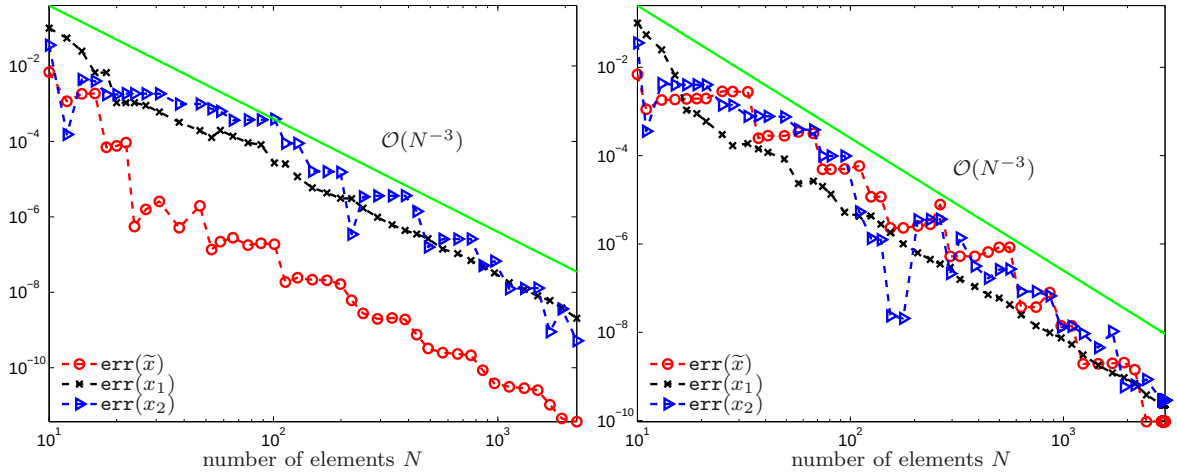

FIGURE 6. Example 7.2: Experimental convergence rates for different point errors at $\widetilde{x} = (-0.24, 0.24)$, $x_1 = (-0.01, -0.01)$, and $x_2 = (-0.24, -0.01)$, where adaptivity with $\theta = 0.4$ and $p = 0$ is driven by Algorithm 3 with respect to only $\widetilde{x}$ (left) and Algorithm 15 (right). The green line indicates the optimal rate of convergence $\mathcal{O}(N^{-3})$.

Example 7.2. Almost-slit domain in 2D. In our second experiment, we study the case of a strong generic singularity. The domain $\Omega \subset \mathbb{R}^2$ shown in Figure 4, has almost a slit; the node indicated by the blue diamond, is $(-0.25, -d)$ with $d = 10^{-4}$. We prescribe the exact solution by (42) which has a severe but generic singularity at the reentrant corner $(0, 0)$. Uniform mesh-refinement leads to generically worst-case order of convergence $\mathcal{O}(N^{-1})$ for the point error $\mathtt{err}_\ell(\widetilde{x})$ as well as the estimator product $\mathtt{est}_\ell(\widetilde{x})$ from (40) and piecewise constant ($p = 0$) as well as piecewise linear ($p = 1$) BEM discretizations; see Figure 4.

The standard adaptive algorithm (Algorithm 15) leads to improved convergence rates for the estimator product $\mathtt{est}$ of approximately $\mathcal{O}(N^{-7/3})$ for $p = 0$ and $\mathcal{O}(N^{-3})$ for

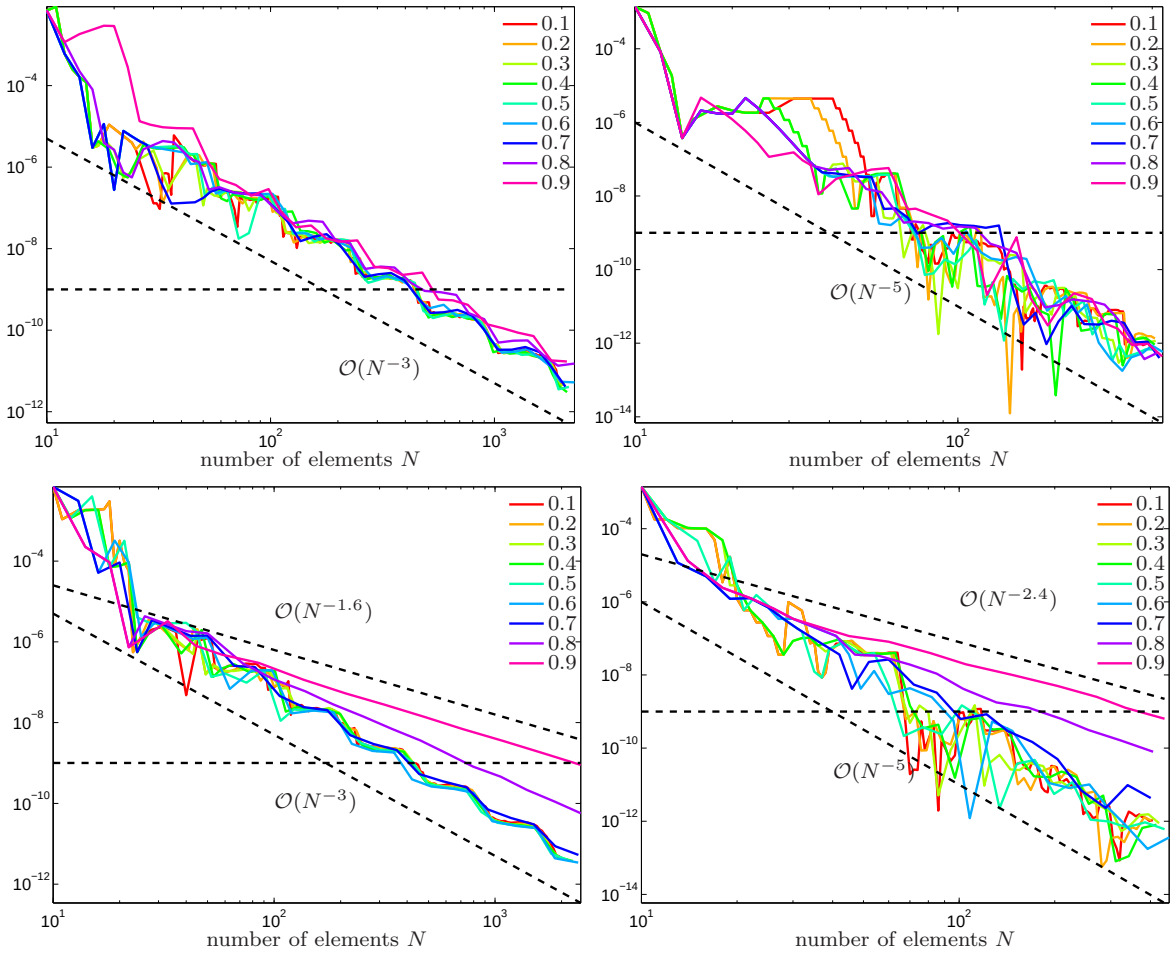

FIGURE 7. Example 7.2: Experimental convergence behavior of Algorithm 1 (top) and Algorithm 3 (bottom) for the point error $\mathtt{err}_\ell(\widetilde{x})$ and different parameters $\theta \in \{0.1, \dots, 0.9\}$: $p = 0$ (left) vs. $p = 1$ (right). The horizontal line at 10^{-9} indicates the tolerance for Table 1.

	$p = 0$			$p = 1$		
θ	Alg. 1	Alg. 3	Alg. 15	Alg. 1	Alg. 3	Alg. 15
0.1	132	82	142	54	47	> 199
0.2	78	51	82	49	39	> 76
0.3	60	37	53	41	23	> 58
0.4	50	29	43	41	21	> 46
0.5	40	23	34	24	17	> 35
0.6	34	19	31	23	16	> 33
0.7	31	17	28	22	15	34
0.8	29	16	27	25	15	33
0.9	27	16	25	22	15	31

TABLE 1. Example 7.2: Number of adaptive steps ℓ to reach a prescribed accuracy 10^{-9} for the point error $\mathtt{err}_\ell(\widetilde{x})$, where $> L$ indicates that the adaptive algorithm did not reach this accuracy within L steps and for less than 2500 ($p = 0$) resp. 500 ($p = 1$) elements..

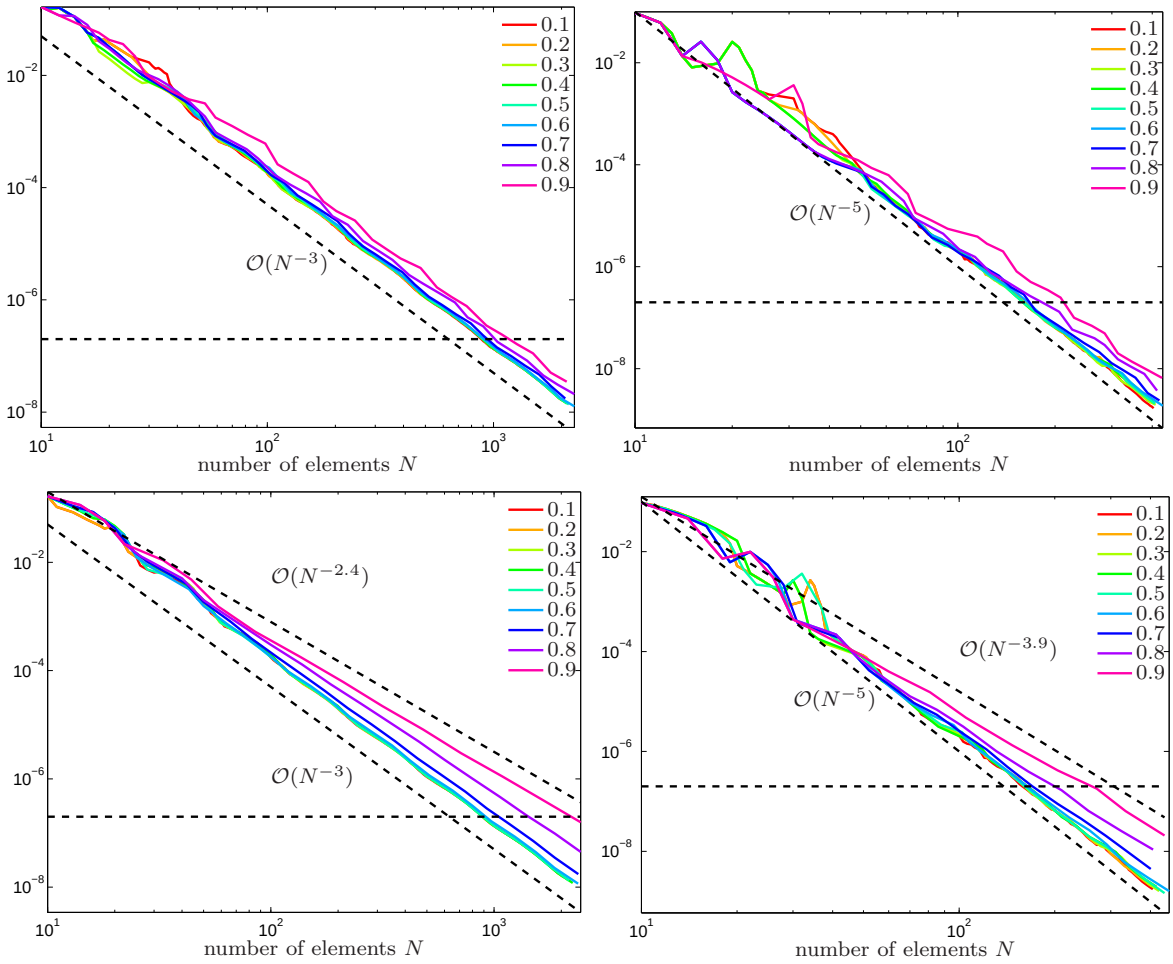

FIGURE 8. Example 7.2: Experimental convergence behavior of Algorithm 1 (top) and Algorithm 3 (bottom) for the estimator product $\mathtt{est}_\ell(\widetilde{x})$ and different parameters $\theta \in \{0.1, \dots, 0.9\}$: $p = 0$ (left) vs. $p = 1$ (right). The horizontal line at 2×10^{-7} indicates the tolerance for Table 2.

	$p = 0$			$p = 1$		
θ	Alg. 1	Alg. 3	Alg. 15	Alg. 1	Alg. 3	Alg. 15
0.1	176	108	158	105	79	> 199
0.2	99	64	> 172	79	57	> 76
0.3	74	44	57	62	35	> 58
0.4	59	35	> 99	54	29	> 46
0.5	47	27	36	36	24	> 35
0.6	40	23	32	33	20	> 33
0.7	37	21	30	31	19	33
0.8	34	19	29	29	15	33
0.9	32	16	> 27	29	13	> 31

TABLE 2. Example 7.2: Number of adaptive steps ℓ to reach a prescribed accuracy 2×10^{-7} for the estimator product $\mathtt{est}_\ell(\widetilde{x})$, where $> L$ indicates that the adaptive algorithm did not reach this accuracy within L steps and for less than 2500 ($p = 0$) resp. 500 ($p = 1$) elements..

$p = 1$, while Algorithm 1 and Algorithm 15 regain the optimal rates $\mathcal{O}(N^{-3})$ for $p = 0$ resp. $\mathcal{O}(N^{-5})$ for $p = 1$; see Figure 5 for $\theta = 0.4$. Other choices of, e.g., $\theta \in \{0.1, 0.2\}$ lead to similar results (not displayed). Moreover, we observe that Algorithm 15 for $p = 1$ even leads to a suboptimal convergence for the point error $\mathtt{err}_\ell(\widetilde{x})$. In addition, we do not only empirically observe optimal convergence rates for $\mathtt{err}_\ell(\widetilde{x})$, where $\psi = \psi[\widetilde{x}]$ drives the adaptivity, but also for other points $x \in \Omega\backslash\{\widetilde{x}\}$ which are formally unknown to the algorithms; see Figure 6.

For Algorithm 1 and Algorithm 3, we study the dependence of optimal convergence rates on the choice of the marking parameter $\theta \in \{0.1, \dots, 0.9\}$ in Figure 7 for the point error $\mathtt{err}_\ell(\widetilde{x})$ and in Figure 8 for the estimator product $\mathtt{est}_\ell(\widetilde{x})$. Unlike Example 7.1, we now observe that Algorithm 1 is more stable in the sense that any choice of θ leads to optimal convergence behavior, while Algorithm 3 appears to be suboptimal for $\theta \geq 0.7$. On the one hand, we note that our analysis only yields optimal convergence of Algorithm 1 for $0 < \theta < \theta_\star < 1$, while for Algorithm 3 we required $0 < \theta < \theta_\star/2$. On the other hand, we underline the observation of [BET11] that Algorithm 3 may lead to a better contraction $0 < q_{\mathrm{lin}} < 1$ in the linear convergence result (30) than Algorithm 1: Table 1 and Table 2 give the number of adaptive steps ℓ to reach a prescribed accuracy 10^{-9} for the point error $\mathtt{err}_\ell(\widetilde{x})$ resp. 2×10^{-7} for the estimator product $\mathtt{est}_\ell(\widetilde{x})$. Throughout, we observe that Algorithm 3 requires much less steps than Algorithm 1 as well as Algorithm 15 (approximately only $50\% - 60\%$ of the steps of Algorithm 1).

Example 7.3. U-shaped domain in 3D. In the final example, we consider the U-shaped domain $\Omega := \big[(-1, 1) \times (-2, 1) \setminus [-1, 0] \times [-1, 0]\big)\big] \times (0, 1) \subset \mathbb{R}^3$ from Figure 9. We prescribe the exact solution

$$u(x, y, z) = z r_1^{2/3} \cos(2/3\varphi_1) + r_2^{2/3} \cos(2/3\varphi_2) \quad \text{in } \Omega \subset \mathbb{R}^3 \tag{43}$$

where (r_1, φ_1, z) resp. (r_2, φ_2, z) denote the cylindrical coordinates of $(x, y, z) \in \mathbb{R}^3$ resp. $(x, y + 1, z) \in \mathbb{R}^3$. We note that u is singular along the reentrant edges $(0, 0, z)$ and $(0, -1, z)$. For the discretization, we use lowest-order BEM ($p = 0$).

The empirical observations are similar to 2D: Uniform mesh-refinement only leads to a rate of convergence $\mathcal{O}(N^{-2/3})$ for the point error $\mathtt{err}_\ell(\widetilde{x})$ as well as the estimator product $\mathtt{est}_\ell(\widetilde{x})$; see Figure 9. Adaptive mesh-refinement improves the convergence rates. While Algorithm 1 and Algorithm 3 lead to approximately $\mathcal{O}(N^{-4/3})$ for the estimator product $\mathtt{est}_\ell(\widetilde{x})$, the standard adaptive strategy of Algorithm 15 only leads to $\mathcal{O}(N^{-1})$; see Figure 10. For the point error $\mathtt{err}_\ell(\widetilde{x})$, either adaptive strategy leads to convergence rate $\mathcal{O}(N^{-4/3})$; see also Figure 11. Empirically, the convergence behavior of Algorithm 1 as well as Algorithm 3 is robust in $\theta \in \{0.1, \dots, 0.9\}$. For all choices of θ, we observe the same convergence rates; see Figure 12. As for Example 7.2, we observe that Algorithm 3 is more effective than Algorithm 1 in the sense that it requires less adaptive steps to reach a prescribed accuracy; see Table 3.

References

[AEF+14] Markus Aurada, Michael Ebner, Michael Feischl, Samuel Ferraz-Leite, Thomas Führer, Petra Goldenits, Michael Karkulik, Markus Mayr, and Dirk Praetorius. HILBERT—a MATLAB implementation of adaptive 2D-BEM. *Numer. Algorithms*, 67(1):1–32, 2014.

[AFF+13] Markus Aurada, Michael Feischl, Thomas Führer, Michael Karkulik, and Dirk Praetorius. Efficiency and optimality of some weighted-residual error estimator for adaptive 2D boundary element methods. *Comput. Methods Appl. Math.*, 13(3):305–332, 2013.

[AFF+14] Markus Aurada, Michael Feischl, Thomas Führer, Michael Karkulik, Jens Markus Melenk, and Dirk Praetorius. invest-paper. 2014.

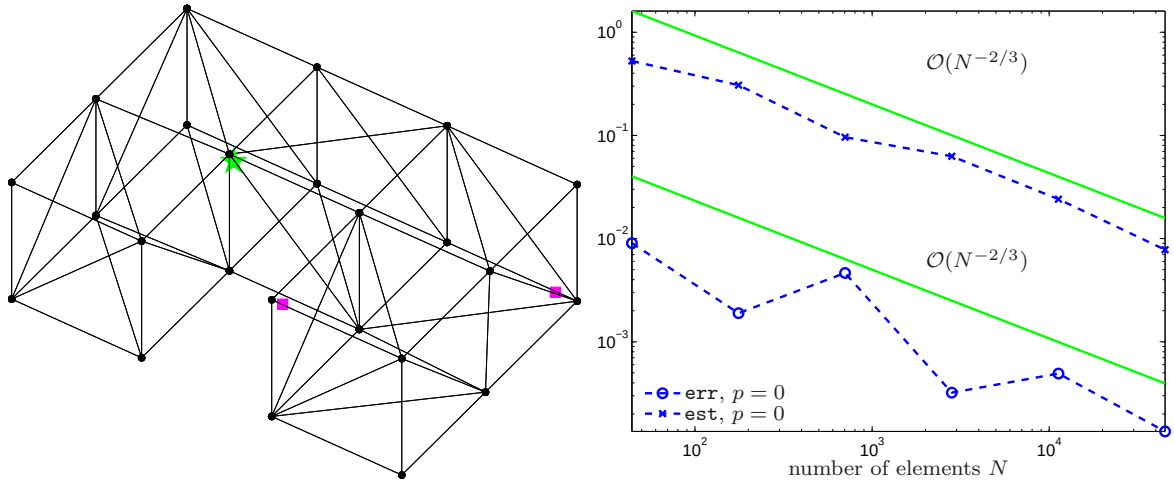

FIGURE 9. Example 7.3: Geometry and initial partition with $N = 56$ surface triangles (left), where the green star indicates the evaluation point $\widetilde{x} = (0.05, 0, 0.9)$. The magenta squares indicate additional evaluation points $x_1 = (0.9, -1.9, 0.1)$ resp. $x_2 = (0.05, -1, 0.5)$, which are not used to steer the adaptive algorithms (left). Uniform mesh-refinement leads to a reduced convergence order of approximately $\mathcal{O}(N^{-2/3})$ for $p = 0$ (right).

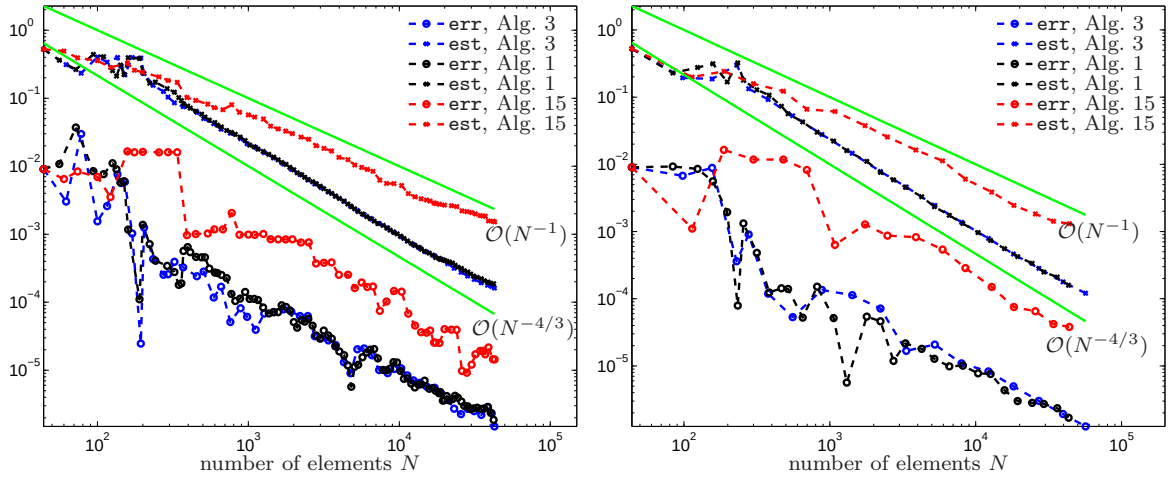

FIGURE 10. Example 7.3: Experimental convergence of adaptive algorithms with $\theta = 0.1$ (left) and $\theta = 0.4$ (right) for $p = 0$. The green lines indicate an improved rate of convergence $\mathcal{O}(N^{-4/3})$ as well as a reduced order of convergence $\mathcal{O}(N^{-1})$ which is observed for Algorithm 15.

[BDD04] Peter Binev, Wolfgang Dahmen, and Ron DeVore. Adaptive finite element methods with convergence rates. *Numer. Math.*, 97(2):219–268, 2004.

[BET11] Roland Becker, Elodie Estecahandy, and David Trujillo. Weighted marking for goal-oriented adaptive finite element methods. *SIAM J. Numer. Anal.*, 49(6):2451–2469, 2011.

[Car97] Carsten Carstensen. An a posteriori error estimate for a first-kind integral equation. *Math. Comp.*, 66(217):139–155, 1997.

[CFPP14] Carsten Carstensen, Michael Feischl, Marcus Page, and Dirk Praetorius. Axioms of adaptivity. *Comput. Math. Appl.*, 67(6):1195–1253, 2014.

[CKNS08] J. Manuel Cascon, Christian Kreuzer, Ricardo H. Nochetto, and Kunibert G. Siebert. Quasi-optimal convergence rate for an adaptive finite element method. *SIAM J. Numer. Anal.*, 46(5):2524–2550, 2008.

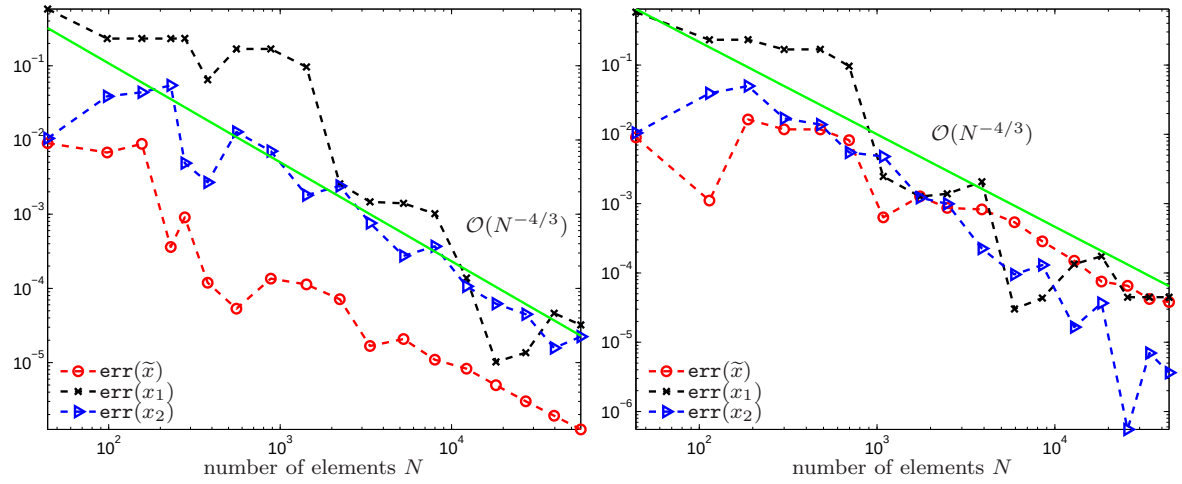

FIGURE 11. Example 7.3: Experimental convergence rates for different point errors at $\widetilde{x} = (0.05, 0, 0.9)$, $x_1 = (0.9, -1.9, 0.1)$, and $x_2 = (0.05, -1, 0.5)$, where adaptivity with $\theta = 0.4$ and $p = 0$ is driven by Algorithm 3 with respect to only $\widetilde{x}$ (left) and the standard algorithm (right). The green line indicates the optimal rate of convergence $\mathcal{O}(N^{-4/3})$.

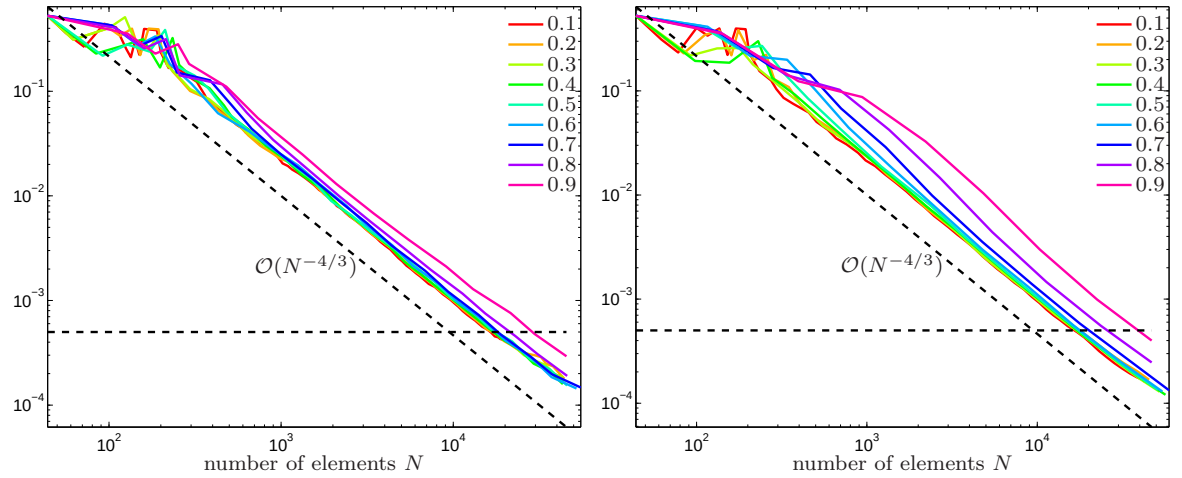

FIGURE 12. Example 7.3: Experimental convergence behavior of Algorithm 1 (left) and Algorithm 3 (right) for the estimator product $\mathtt{est}_\ell(\widetilde{x})$ and different parameters $\theta \in \{0.1, \dots, 0.9\}$ with $p = 0$. The horizontal lines at 5×10^{-4} indicate the tolerance for Table 3.

[CMS01] Carsten Carstensen, Matthias Maischak, and Ernst P. Stephan. A posteriori error estimate and h-adaptive algorithm on surfaces for Symm's integral equation. *Numer. Math.*, 90(2):197–213, 2001.

[FFK+13] Michael Feischl, Thomas Führer, Michael Karkulik, Jens Markus Melenk, and Dirk Praetorius. Quasi-optimal convergence rates for adaptive boundary element methods with data approximation, Part II: Hyper-singular integral equation. *ASC Report*, 30/2013, 2013.

[FFK+14] Michael Feischl, Thomas Führer, Michael Karkulik, Jens Markus Melenk, and Dirk Praetorius. Quasi-optimal convergence rates for adaptive boundary element methods with data approximation, Part I: Weakly-singular integral equation. *Calcolo*, in print, 2014.

[FKMP13] Michael Feischl, Michael Karkulik, Jens Markus Melenk, and Dirk Praetorius. Quasi-optimal convergence rate for an adaptive boundary element method. *SIAM J. Numer. Anal.*, 51(2):1327–1348, 2013.

θ	Alg. 1	Alg. 3	Alg. 15
0.1	82	49	> 61
0.2	52	7	> 30
0.3	35	19	> 22
0.4	26	15	> 17
0.5	23	14	> 13
0.6	20	12	> 12
0.7	19	11	> 11
0.8	17	10	> 10
0.9	15	9	> 9

θ	Alg. 1	Alg. 3	Alg. 15
0.1	81	48	> 61
0.2	47	28	> 30
0.3	34	18	> 22
0.4	27	15	> 17
0.5	23	13	> 13
0.6	19	12	> 12
0.7	17	11	> 11
0.8	16	10	> 10
0.9	15	9	> 9

TABLE 3. Example 7.3: Number of adaptive steps ℓ to reach a prescribed accuracy 10^{-7} for the point error $\mathtt{err}_\ell(\widetilde{x})$ (left) resp. a prescribed accuracy 5×10^{-5} for the estimator product $\mathtt{est}_\ell(\widetilde{x})$ (right), where $> L$ indicates that Algorithm 15 did not reach this accuracy within L steps and for less than 42.000 elements.

[FPV14] Michael Feischl, Dirk Praetorius, and Kristoffer Van Der Zee. An abstract analysis of optimal goal-oriented adaptive FEM and application to second-order linear elliptic PDEs. *in preparation*, 2014.

[Gan13] Tsogtgerel Gantumur. Adaptive boundary element methods with convergence rates. *Numer. Math.*, 124(3):471–516, 2013.

[HW08] George C. Hsiao and Wolfgang L. Wendland. *Boundary integral equations*, volume 164 of *Applied Mathematical Sciences*. Springer-Verlag, Berlin, 2008.

[KPP13] Michael Karkulik, David Pavlicek, and Dirk Praetorius. On 2D newest vertex bisection: optimality of mesh-closure and H^1-stability of L_2-projection. *Constr. Approx.*, 38(2):213–234, 2013.

[McL00] William McLean. *Strongly elliptic systems and boundary integral equations*. Cambridge University Press, Cambridge, 2000.

[MS09] Mario S. Mommer and Rob Stevenson. A goal-oriented adaptive finite element method with convergence rates. *SIAM J. Numer. Anal.*, 47(2):861–886, 2009.

[NV12] Ricardo H. Nochetto and Andreas Veeser. Primer of adaptive finite element methods. Naldi, Giovanni (ed.) et al., Multiscale and adaptivity: Modeling, numerics and applications. C.I.M.E. summer school, Cetraro, Italy, July 6–11, 2009. Berlin: Springer; Firenze: Fondazione CIME Roberto Conti. Lecture Notes in Mathematics 2040, 125-225 (2012), 2012.

[SAB+14] Wojciech Smigaj, Simon Arridge, Timo Betcke, Joel Phillips, and Martin Schweiger. Solving boundary integral problems with BEM++. *ACM Trans. Math. Software*, to appear, 2014.

[SS11] Stefan A. Sauter and Christoph Schwab. *Boundary element methods*, volume 39 of *Springer Series in Computational Mathematics*. Springer-Verlag, Berlin, 2011. Translated and expanded from the 2004 German original.

[Ste07] Rob Stevenson. Optimality of a standard adaptive finite element method. *Found. Comput. Math.*, 7(2):245–269, 2007.

[Ste08] Olaf Steinbach. *Numerical approximation methods for elliptic boundary value problems*. Springer, New York, 2008. Finite and boundary elements, Translated from the 2003 German original.